J Exp Biol Advance Online Articles. First posted online on 19 June 2014 as doi:10.1242/jeb.105098
Access the most recent version at http://jeb.biologists.org/lookup/doi/10.1242/jeb.105098

Aquaporin expression in the Japanese medaka (*Oryzias latipes*, Temminck & Schlegel) in FW and SW: challenging the paradigm of intestinal water transport?

Steffen S. Madsen[1,2,*], Joanna Bujak[2] and Christian K. Tipsmark[2]

[1]Department of Biology, University of Southern Denmark, DK-5230 Odense M, Denmark.

[2]Department of Biological Sciences, University of Arkansas, SCEN601, Fayetteville, AR72701, USA.

*) author for correspondence (steffen@biology.sdu.dk)

Abstract

We investigated the salinity dependent expression dynamics of 7 aquaporin paralogs (*aqp1a, -3a, -7, -8ab, -10a, -10b* and *-11a*) in several tissues of euryhaline Japanese medaka (*Oryzias latipes*). All paralogs except *aqp7* and *-10a* had a broad tissue distribution and several were affected by salinity in both osmoregulatory and non-osmoregulatory tissues. In the intestine, *aqp1a, -7, -8ab* and *-10a* decreased upon seawater (SW)-acclimation in both long-term acclimated fish and during 1-3 days of the transition period. In the gill, *aqp3a* was lower and *aqp10a* higher in SW than in freshwater (FW). In the kidney no *aqps* were affected by salinity. In the skin, *aqp1a* and *-3a* were lower in SW than in FW. In the liver *aqp8ab* and *-10a* were lower in SW than in FW. Further, 6 Na^+,K^+-ATPase α-subunit isoform transcripts were analyzed in the intestine but none showed a consistent response to salinity, suggesting that water transport is not regulated at this level. In contrast, mRNA of the Na^+,K^+,$2Cl^-$-cotransporter type-2 strongly increased in the intestine in SW compared to FW fish. Using custom made antibodies, Aqp1a, -8ab and -10a were localized in the apical region of enterocytes of FW fish. Apical staining intensity strongly decreased, vanished or moved to sub apical regions, when fish were acclimated to SW, supporting the lower mRNA expression in SW. Western blots confirmed the decrease in Aqp1a and -10a in SW. The strong decrease in aquaporin expression in the intestine of SW fish is surprising and challenges the paradigm for transepithelial intestinal water absorption in SW fishes.

Key words: Aquaporin, intestine, salinity, water transport

Introduction

Teleost osmoregulation has been the focus of hundreds of papers since the pioneering studies of Homer W. Smith, August Krogh and colleagues in the 1930s (Smith, 1929; Krogh, 1937). This has led to several models describing the overall mechanisms as well as molecular details of the major osmoregulatory organs, such as gill, kidney and intestine. Based on relatively few euryhaline "model" species (rainbow trout, eel, killifish, tilapia) consensus models have been established on many of the detailed osmoregulatory mechanisms used by euryhaline teleosts when living in freshwater (FW) and seawater (SW) and during transitions between the two extremes. In FW, hyper-osmoregulatory mechanisms involve active ion uptake in the gill and excretion of copious amounts of hypotonic urine in order to compensate for passive ion loss to and water load from the environment. In SW, drinking and intestinal absorption of hyper-isotonic salt water in combination with branchial excretion of monovalent ions comprise the general hypo-osmoregulatory mechanisms that compensate for passive dehydration and ion-load from the environment. Most studies have focused on the pathways of ionic regulation involving membrane bound ion-channels, -exchangers, active mechanisms and intercellular tight junctions, which has given rise to advanced diagrams of the molecular pathways involved in ion transport (see Grosell 2011; Hwang *et al*., 2011). Much less attention has been paid to the molecular pathways involved in the exchange of water across epithelial barriers.

Theoretically, water may pass epithelia such as the intestinal mucosa by three pathways: simple diffusion through lipid bilayers, paracellular diffusion through apical tight junctions, or transcellular passage mediated by specific carriers such as aquaporins or alternative proteins such as the sodium-glucose transporter (Loo *et al*., 2002) or the Na^+,K^+,2Cl^--cotransporter (Hamann *et al*., 2005). Irrespective of mechanism, there is consensus that water is transported by solute-linked transport based on Diamond and Bossert's (1967) "standing gradient model" (Larsen and Møbjerg, 2006). This means that a local osmotic gradient needs to be established in order to drive the flux of water, and that the Na^+,K^+-ATPase is an important component of this by its contribution to NaCl accumulation in the lateral intercellular space. SW-acclimation in fishes is associated with increased drinking, esophageal or intestinal desalination and subsequent isotonic intestinal water absorption (Grosell, 2011). Most current evidence points to a transcellular route for water absorption (Sundell and Sundh, 2011; Wood and Grosell, 2012).

Our knowledge about aquaporins in fish is still rather fragmentary and gathered from a few steno- and euryhaline species. In the genome of the stenohaline FW zebrafish, *Danio rerio*, 11 aquaporin

subfamilies are present, representing mammalian isoforms AQP0-1, 3-5 and 7-12. Some of these have duplicate or triplicate paralogs leading to a total of 18 paralogs (Cerdà and Finn, 2010). Thus the situation in fishes is quite a bit more complex than in mammals, where 13 isoforms (AQP0-12) are present, each represented by only one paralog (King *et al*., 2004). Tetrapod aquaporin proteins may generally be divided into 3 subfamilies based on their transport characteristics: true water permeable aquapores (AQP0-2,4-6,8), the aqua-glyceropores (AQP3,7,10) with additional permeabilities to glycerol and urea and the unorthodox or super-aquaporins (AQP11-12), with yet poorly defined permeability characteristics. When comparing different teleosts, several aquaporin paralogs are associated with the gastro-intestinal tissues: Aqp1aa/ab, -3a, -4, -7, -8aa/ab, -10a/b, -11b and -12 (see Cerdà and Finn, 2010); but at closer look only Aqp1aa/ab, and -8ab have been convincingly demonstrated in the mucosal, enterocytic cell layer of various teleosts (Atlantic salmon, *Salmo salar*: Madsen *et al*., 2011; European eel, *Anguilla anguilla*: Martinez *et al*., 2005; Japanese eel, *A. japonica*: Aoki *et al*., 2003; gilthead seabream, *Sparus aurata*: Raldúa *et al*., 2008). All other paralogs have either not been investigated yet or identified in other cell types. The contribution of aquaporins to intestinal water transport in fishes has only been little studied. In most species investigated (Japanese and European eel, Atlantic salmon, sea bream, European sea bass (*Dicentrarchus labrax*) SW-acclimation is accompanied by increased expression of these paralogs, suggesting a role in creating the transcellular water absorption pathway (Aoki *et al*., 2003; Martinez *et al*., 2005; Giffard-Mena *et al*., 2007, 2008; Raldúa *et al*., 2008; Tipsmark *et al*., 2010b). Due to the variety of paralogs present in teleosts, there is a need to systematically investigate the dynamics, localization and properties of each in order to understand their role in transcellular water transport vs. cellular volume regulation. There is also a need to include alternative euryhaline species to unravel general as well as species-specific patterns. On such species is the Japanese medaka (*Oryzias latipes*; Inoue and Takei, 2003). It belongs to the family of Ricefishes (*Adrianichthyidae*; Order: *Beloniformes*) and has been used in several genetic and developmental studies (Ishikawa, 2000). Some of its advantages are: it is a highly euryhaline FW teleost (Sakamoto *et al*., 2001); it is a small fish, relatively easy to breed and rear, and its genome is fully sequenced, annotated and is relatively small (800 Mb) compared to other model species (Tanaka, 1995). Thus, this species is well suited for genetic manipulation experiments including transgenic and knock-down techniques. An additional advantage is the presence of 30 related species for phylogenetic comparisons of the development of salinity tolerance (www.fishbase.org/). The Japanese medaka can handle direct transfer from FW to 30 ppt SW and regain osmotic homeostasis after less than 1 day (Sakamoto *et*

al., 2001; Kang *et al*., 2008), even though step-wise transfer to brackish water may increase its performance prior to transfer to full strength SW (Inoue *et al*., 2003). Gill Na^+,K^+-ATPase abundance and gill filament chloride cell density and size is higher in SW than FW (Sakamoto *et al*., 2001; Kang *et al*., 2008), and medaka larvae increased drinking rate when transferred from FW to 80% SW (Kaneko and Hasegawa, 1999). Thus the available information suggests that Japanese medaka responds to salinity change mostly similar to other well-described euryhaline teleosts. However, in order to fully benefit from the advantages of using medaka as a euryhaline model fish and to apply more advanced molecular techniques, there is a need to gather information on transcriptomic and proteomic aspects of osmoregulation.

Our objective was to first characterize and compare the tissue expression pattern of aquaporin paralogs suspected to be involved in osmoregulation in the Japanese medaka. With focus on the intestine, we then wanted to characterize aquaporin expression dynamics in fish acclimating between FW and SW. Based hereupon we developed homologous antibodies to those aquaporins showing a salinity response and characterized the dynamics and localization in the intestine also at the protein level. Our working hypothesis was that selected aquaporins become functionally more abundant in the intestine, when fish are moved to a hyperosmotic medium.

Results

Aquaporin and NKCC2 transcript tissue distribution.

The transcripts of seven aquaporin paralogs were analyzed in 9 different tissues in long-term FW- and SW-acclimated medaka (Fig. 1). All paralogs were ubiquitously expressed (above detection level) in both osmoregulatory and non-osmoregulatory tissues. However, there were major differences in expression levels among tissues (range of the observed Ct values was: Aqp1a: 20-29, Aqp3a: 18-30, Aqp7: 23-31, Aqp8ab: 22-33; Aqp10a: 19-34; Aqp10b: 22-30; Aqp11: 24-27). *aqp1a*: Highest expression in intestine, spleen and kidney followed by muscle, liver and brain. *aqp3a*: Highest expression in skin, followed by gill and muscle. *aqp7*: Highest expression in liver, followed by spleen, intestine and gonad. *aqp8ab*: Highest expression in intestine, more than 40x higher than spleen, gill and additional tissues. *aqp10a*: Highest expression in intestine, more than 40x higher than liver, brain. *aqp10b*: Highest expression in intestine, roughly 10x or more than in all other tissues. *aqp11a*: Relatively ubiquitous distribution. *NKCC2*: Almost exclusively expressed in intestine and kidney.

Salinity affected the expression level in several cases (Fig. 1): *aqp1a*: Lower level in SW intestine (1/5x) and skin (1/3x), than in corresponding FW samples. *aqp3a:* Lower level in SW skin (1/3x), gonad (1/7x) and gill (1/8x) compared to FW samples. *aqp8ab:* Lower level in SW intestine (1/5x) and liver (1/5x) than in FW samples. *aqp10a:* Lower level in SW intestine (1/80x) and liver (1/75x) than in FW samples; higher level in SW gill (8x) than in FW samples. *NKCC2:* Higher level in SW intestine (>5x) and gonads (>45x) than in FW samples; lower level in SW kidney (1/5x) than in FW samples.

Short term salinity transfer experiments

FW-SW-transfer: Muscle water decreased 24 h after FW-SW transfer but was re-established after 72 h (Fig. 2H). In the intestine, SW-transfer induced a consistent overall decrease in the transcript level of *aqp1a, -7, -8ab* and *-10a*, whereas *aqp3a, -10b* and *-11a* levels were unaffected (Fig. 2). Furthermore, the transcript level of six isoforms of the Na^+,K^+-ATPase α-subunit were investigated in the intestine (Fig. 3). Only the α2-subunit showed an overall response to salinity and was lower in SW than in FW. The remaining isoforms showed either no response, a time effect and/or a time x salinity interaction. The NKCC2 showed a strong increase after SW-transfer (Fig- 3G) whereas the SGLT1 showed a time effect.

SW-FW-transfer: Muscle water did not respond to SW-FW transfer within the time frame of sampling (Fig. 4H). In the intestine, FW-transfer induced a consistent overall increase in the transcript level of *aqp1a, -8ab* and *-10a*, whereas *aqp3a, -7, -10b* and *-11a* were unaffected (Fig. 4). None of the Na^+,K^+-ATPase alpha subunit isoforms responded consistently to the transfer (Fig. 5). The NKCC2 on the other hand showed a strong and lasting decline after transfer to FW (Fig. 5G). The SGLT1 did not respond to the transfer (Fig. 5H).

Western blotting and antibody validation

Western blots of intestinal membrane fractions probed with Aqp1a, -8ab and -10a affinity purified antibodies revealed immunoreactive bands around 25, 28 and 35 kDa, respectively (Fig. 6). For Aqp8ab there were two additional bands around 30-35 kDa. For all three antibodies, neutralization with 400-fold molar excess of the respective antigenic peptide blocked the immunoreactivity band. Semi-quantitative Western blotting revealed that Aqp1a and -10a protein levels in intestinal membrane fractions from SW-acclimated fish were significantly lower than the level in

corresponding FW samples (Fig. 8). By comparison, there was no difference in the level of Aqp8ab protein between FW and SW samples.

Immunofluorescence microscopy

All three aquaporin antibodies gave a distinct and almost exclusive apical - presumably brush border staining of intestinal tissue of FW fish (Fig. 8-10, red color). Even though the staining intensity varied slightly along the brush border it appeared very similar for the three antibodies. There was very little and only sporadic staining of the intracellular compartment with any Aqp antibody. The apical staining was absent (Aqp10a), much reduced or withdrawn to the cytosolic compartment (Aqp1a and Aqp8ab) when analyzing SW-acclimated fish. The α5 Na^+,K^+-ATPase alpha subunit antibody (green color) produced lateral and basolateral staining typical of membranous enterocytic cells. This staining was absent from the apical brush border and cytosolic part of the cells. There was no obvious difference in staining intensity when comparing FW and SW fish.

Electrophysiology

The transepithelial resistance (TER) of the intestine was generally very low (3-12 Ω*cm^2, Table 1). There was no effect of acclimation salinity on TER but there was a significant effect of region with the anterior segments having a higher TER than the posterior segments.

Discussion

In the genome of the Japanese medaka we identified 13 annotated sequences of aquaporin paralogs (Tingaud-Sequeira *et al*., 2010): Aqp0a, -0b, -1a, -3a, -4, -7, -8ab, -9, -10a, -10b, -11a, 11b and -12. This is less than the 18 paralogs found in zebrafish, which was expected due to the much smaller genome of medaka compared to zebrafish. All 13 medaka sequences were previously shown in a phylogenetic analysis to group with the related and cloned paralogs from several other teleosts including zebrafish (Tingaud-Sequeira *et al*., 2010) and the marine medaka, *O. dancena* (Kim *et al*., 2014). We investigated the tissue distribution and salinity response of seven of these (*aqp1a, -3a, -7, -8ab, -10a, -10b, -11a*), based on our expectation of a particular role in water transport in the intestine and other osmoregulatory tissues. Our data show that most paralogs are expressed in many tissues, even though in some cases there is a pronounced (100-1000 fold) difference in the transcript level. Thus aquaporins are not confined to osmoregulatory tissues but may also occur relatively

highly expressed in liver, spleen, skin and gonadal tissue. Some aquaporin transcripts responded strongly to ambient salinity both in short- and long-term experiments. This was predominant in the intestine but also in skin, gill and liver, whereas none of the paralogs respond to salinity in the kidney. A remarkable finding of the study is that three of the predominant paralogs in the intestine (Aqp1a, -8ab, and -10a) decrease when fish were transferred to a hyperosmotic medium, which is opposite to our hypothesis and to most other studies of euryhaline fishes. This finding is a challenge to the paradigm for how intestinal water absorption occurs in SW-acclimated fishes.

Tissue distribution of aquaporins and NKCC2

Several studies reported on expression and modulation by salinity of aquaporins in teleost osmoregulatory tissues (see Cerda and Finn, 2010). However, information on AQP expression in non-osmoregulatory tissues is limited. AQP1 is a true water pore, and is the most ubiquitously expressed aquaporin in mammals (Ishibashi *et al*., 2009). In Japanese medaka, *aqp1a* was most abundant in the intestine, spleen and kidney but also present at lower levels in all other tissues examined, which in part may reflect its general expression in erythrocytes and endothelial barriers (Mobasheri and Marples, 2004). This ubiquitous tissue distribution is in accordance with zebrafish, sea bream, Atlantic salmon and European eel, and marine medaka (Fabra *et al*., 2005; Martinez *et al*., 2005; Tingaud-Sequeira *et al*., 2010; Tipsmark *et al*., 2010b; Kim *et al*., 2014). The role of Aqp1a in osmoregulatory tissues is most likely linked to transepithelial water transport, whereas its physiological role in other tissues is unknown. Aquaporins in the spleen have been speculated to be involved in the trafficking of hemapoietic cells (Tyagi and Tangevelu, 2010).

aqp3a, an aqua-glyceropore, was present at highest levels in skin and gill, which was also the case in tilapia (*Oreochromis mossambicus*: Watanabe *et al*., 2005) and in marine medaka (Kim *et al*., 2014). In these two tissues, both directly exposed to the external medium, the transcript level was 8-10-fold higher in FW than in SW. Interestingly, in mammals AQP3 is localized in the basal epidermal cell layer, where it has been proposed a role in skin hydration via its glycerol transporting properties (see Hara-Chikuma and Verkman, 2006). A relatively high level was also found in muscle, in accordance with Atlantic salmon and marine medaka (Tipsmark *et al*., 2010b; Kim *et al*., 2014) but at variance with mammals, where AQP3 is not expressed in muscle (Ishibashi *et al*., 2009). The overall tissue distribution in Japanese medaka is well in accordance with that reported in zebrafish (Tingaud-Sequeira *et al*., 2010) and tilapia (Watanabe *et al*., 2005). In the gill, Aqp3 has been localized specifically in the basolateral membrane of chloride cells in the European eel

(*aqp3b*: Cutler and Cramb, 2002; Lignot *et al*., 2002), Japanese eel (Tse *et al*., 2006), sea wrasse (*Coris julis*: Brunelli *et al*., 2010), sea bass (Giffard-Mena *et al*., 2007, 2008), silver sea bream (*S. sarba*: Deane and Woo, 2006), tilapia (*aqp3a*: Watanabe *et al*., 2005) and killifish (*Fundulus heteroclitus*: Jung *et al*., 2012), where the mRNA level is higher in FW than SW-acclimated fish, thus in accordance with our data. The localization in the basolateral membrane agrees with its proposed role as an osmosensor involved in cellular volume regulation. In contrast, the *aqp3b*-like paralog was recently found to be higher expressed in SW than in FW-acclimated parr gills of sockeye salmon (*Oncorhynchus nerka*: Choi *et al*., 2013). This salinity response was, however, opposite at the smolt stage.

The aqua-glyceropore *aqp7* had the highest expression in liver followed by intestine, spleen and gonadal tissue. The high expression in liver suggests an important role in hepatocyte glycerol metabolism. Among fishes, this paralog has only been reported in zebrafish, where the transcript was present in intestine, gonads, gills, kidney and skin but absent in the liver as judged by RT-PCR (Tingaud-Sequeira *et al*., 2010). In mammals, AQP7 has a relatively narrow tissue distribution, and focus has been on the role as a glycerol channel in association with adipose and liver tissue (Rodríguez *et al*., 2011). AQP7 is also expressed in the apical brush border of the rat small intestine, where it may have a role in water movement in the apical domain of enterocytes (Laforenza *et al*. 2005); in the apical membrane of rat proximal straight tubules, where its role may be in water absorption or urea secretion, thus participating in the concentrating mechanism of the mammalian kidney (Ishibashi *et al*., 2000a); and finally, AQP7 was localized in the plasma membrane of skeletal muscle fibers (Wakayama *et al*., 2004), where its function is yet unknown.

aqp8ab is one of several *aqp8* paralogs that has been reported in fish, though in most cases it is unclear which paralog is reported: Japanese eel *aqp8aa*-like (Kim *et al*., 2010), zebrafish *aqp8aa*, *-8ab*, *-8b* (Tingaud-Sequeira *et al*., 2010), sockeye salmon Aqp8b-like (Choi *et al*., 2013), Atlantic salmon *aqp8aa*, *-8ab*, *-8b* (Engelund *et al*., 2013). In Japanese medaka, only the Aqp8ab paralog is present in the genome and it is predominantly expressed in the intestine. This is in accordance with Atlantic salmon, where *aqp8ab* is exclusively expressed throughout the intestine and with zebrafish, where the paralog is also strongly expressed in the kidney. In the related marine medaka, *aqp8(ab)* is expressed in intestine but also at relatively high levels in spleen, kidney, and heart (Kim *et al*., 2014). In zebrafish and Atlantic salmon Aqp8ab is permeable to water and urea, and in the salmon it has additional permeability to glycerol, which has not yet been reported in any other species

(Tingaud-Sequeira *et al*., 2010; Engelund *et al*., 2013). In these species at least two additional Aqp8 paralogs exist: Aqp8aa and Aqp8b, with different tissue distribution and transporting capacities compared with Aqp8ab (Engelund *et al*., 2013). In mammals the AQP8 ortholog is expressed in proximal kidney tubules, hepatocytes, testes, salivary gland and intestine (Elkjær *et al*., 2001). In some species it is permeable to urea (Ma *et al*., 1997) and ammonia (Saparov *et al*., 2007) in addition to water but its transport capacity is still debated.

AQP10 is an aqua-glyceropore, which is almost exclusively expressed in regions of the gastro-intestinal tract in human (Hatakeyama *et al*., 2001; Ishibashi *et al*., 2002). Its subcellular localization is controversial (Hatakeyama *et al*., 2001; Ishibashi *et al*., 2002; Mobasheri *et al*., 2004; Li *et al*., 2005; Laforenza *et al*., 2010), and surprisingly, it is a pseudogene in mouse (Morinaga *et al*., 2002). The AQP10 protein was reported in the brush-border membrane of absorptive enterocytes of the upper villus (Mobasheri *et al*.; 2004; Laforenza *et al*.; 2010), whereas other authors have demonstrated the presence of two AQP10 isoforms, one located in gastro-entero-pancreatic endocrine cells and another truncated form (named AQP10v), in capillary endothelial cells of villi (Li *et al*., 2005). In humans, zebrafish and eel the ortholog is permeable to water, glycerol and urea (Ishibashi *et al*., 2002; MacIver *et al*., 2010; Tingaud-Sequeira *et al*., 2010). Recently, it was also found in human adipocytes, where it is co-expressed with two other glyceropores, AQP3 and -7 (Rodríguez *et al*., 2011; Laforenza *et al*., 2013), and may have a major role in glycerol metabolism. In the Japanese medaka, two paralogs are present: *aqp10a* and *-10b*. Both had a relatively narrow tissue distribution most highly expressed in intestine and liver, the latter suggests an important role in glycerol metabolism. In zebrafish, both paralogs are also present: *aqp10a* in the intestine, liver, kidney and gill (Tingaud-Sequeira *et al*., 2012), *aqp10b* in the intestine, kidney (sea bream: Santos *et al*., 2004; eel: Martinez *et al*., 2005; Atlantic salmon: Tipsmark *et al*., 2010b) and gonads (zebrafish: Tingaud-Sequeira *et al*., 2010). In the marine medaka an *aqp10a*-like paralog was reported at relatively high levels in the intestine, ovary, kidney and gill but at very low levels in the liver (Kim *et al*., 2014). The Aqp10b paralog present in sea bream and eel does not seem to play a role in transepithelial water transport as it is expressed mainly in cell layers below the apical enterocytes (Santos *et al*., 2004) and is unresponsive to salinity (Martinez *et al*., 2005). In salmon, *aqp10b* increased after SW-transfer in the middle intestine (Tipsmark *et al*., 2010b). In contrast, the present study suggests that the alternative paralog, Aqp10a, has an important role in water transport, since it was strongly expressed in enterocytes and localized in the brush border membrane.

AQP11 belongs to the subfamily of unorthodox aquaporins with divergent NPA motifs. Its transport properties are controversial, even though low water transport has been reported (Yakata *et al*., 2007). In Japanese medaka, *aqp11a* had a ubiquitous tissue distribution like in the marine medaka (Kim *et al*., 2014) with somewhat higher levels in the intestine, liver and kidney. In zebrafish, *aqp11b* was found only in the gastro-intestinal tract, ovary and liver and absent in kidney (Tingaud-Sequeira *et al*., 2010). In rat, AQP11 also has a broad tissue distribution (Ishibashi *et al*., 2000b) and is localized intracellularly, most likely in association with the endoplasmic reticulum and derived vesicles with a suspected role in vesicular or vacuolar water transport (Morishita *et al*., 2005). Morpholino knock-down of *aqp11* in developing zebrafish embryos causes malformation of the normal linear body shape (Ikeda *et al*., 2011), suggesting a crucial role in morphogenesis.

Two distinct isoforms of NKCC cotransporters (NKCC1 and NKCC2) have been cloned from mammals and fish (Russell, 2000). NKCC1, generally called the secretory isoform, is considered a house-keeping transporter in many cell types (Isenring *et al*., 1998) and is localized in the basolateral membrane of secretory epithelial cells such as the SW gill chloride cells (Evans *et al*., 2005). We analysed *NKCC2*, an absorptive-type cotransporter, which is located apically in kidney tubule cells and enterocytes of mammals (Lytle *et al*., 1996, Xue *et al*., 2009), where it is responsible for a significant proportion of apical sodium absorption. In accordance with marine medaka *(*Kang *et al*., 2010), the expression of NKCC2 in Japanese medaka was several-fold higher in kidney and intestine than in any other tissue analyzed. Furthermore, the transcript increased in the kidney in FW and in the intestine in SW in line with its recognized role in hypo-tonic urine production in FW and intestinal salt absorption in SW, respectively. The absorptive isoform, NKCC2, has been found in the intestine and kidney of many teleosts (winter flounder, *Pseudopleuronectes americanus*: O'Grady *et al*., 1986; Olive flounder, *Paralichythys olivaceus*: Kim *et al*., 2013; rainbow trout, *O. mykiss*, Aguenaou *et al*., 1989; eel Cutler and Cramb, 2002; Watanabe *et al*., 2011). In addition to its main function as carrier of Na^+, K^+ and Cl^- transport, the NKCC1 isoform may also transport significant amounts of water (Hamann *et al*., 2005).

Another potential route for water entry across the apical membrane is the sodium/glucose cotransporter SGLT1, which has been proposed to be a low conductance water channel (Loo *et al*., 1996, 1999). This transporter is present in the apical brush border of rainbow trout (Polakof *et al*., 2010) and Atlantic salmon intestine (Madsen *et al*., 2011), where its inhibition with phloridzin

reduced water transport by 20%. The SGLT1 was also expressed in the medaka intestine but did not show any consistent response to environmental salinity in the present study.

Aquaporin localization, abundance and response to environmental salinity.

Antibodies were generated against the three abundant intestine aquaporins -1a, -8ab and -10a, which all showed a marked decrease in SW at the transcript level. The three antibodies identified protein bands around 25, 30 and 32 kDa, respectively in addition to a duplet around 30-35 kDa in the case of Aqp8ab. These molecular weights match the expected native molecular weights of 25.1, 27.3 and 27.9 kDa for the three aquaporins. The additional duplet may represent glycosylated forms as reported for other aquaporins (Hendriks *et al*., 2004; Pandey *et al*., 2010). The successful blocking of these bands with the respective antigenic peptides validated the specificity of the antibodies.

All three antibodies gave strong immunostaining of the apical region of enterocytes in FW-acclimated medaka. The staining pattern was more or less identical for the three antibodies, suggesting that Aqp1a, -8ab and -10a are all expressed in the apical brush border of the intestine. For unknown reasons, the staining of Aqp8ab was more variable along the brush border than in the case of Aqp1a and -10a. As expected, the alpha-5 antibody produced a strong staining of basolateral membranes indicative of the abundance of Na^+,K^+-ATPase enzyme. There was no sign that this staining intensity was altered by salinity. According to "the standing gradient model" (Larsen and Møbjerg, 2006), the Na^+,K^+-ATPase is the primary driving force for water transport, which is tightly linked to the creation of ionic and osmotic gradients between the lumen and the lateral intercellular space. There was a remarkable decrease in the apical brush border staining for aquaporins, when medakas were acclimated to SW, indicating that the aquaporin proteins were removed from the apical membrane. Retraction from the membrane was accompanied by a more pronounced cytosolic staining in the apical region of enterocytes, especially for Aqp1a and -8ab, suggesting that an internalization of apical membrane domains took place. This observation was supported by the reduced abundance of Aqp1a and -10a in intestinal membrane fractions from SW fish when assayed by Western blotting, and was in line with the much reduced transcript levels of the two aquaporins during acclimation from FW-SW. Aqp8ab on the other hand declined at the transcript level and also disappeared from the apical membrane in SW; however, total Aqp8ab abundance did not change in Western analysis, suggesting that both apical and internalized pools of Aqps were estimated to some degree in the procedure. The removal or internalization of aquaporins

from the apical brush border upon SW-acclimation is surprising, and in contrast to most other studies of aquaporin dynamics in euryhaline fish. In Atlantic salmon (Engelund *et al*., 2013), eel (Aoki *et al*., 2003; Martinez *et al*., 2005), sea bass (Giffard-Mena *et al*., 2007, 2008) and sea bream (Raldúa *et al*., 2008) Aqp1 and -8ab paralogs have been shown to increase in intestinal segments, when fish are acclimated to SW, an observation which is functionally linked to the increased water transport capacity and increased drinking in SW-acclimated fish. Recently, however, decreased intestinal mRNA levels of *aqp8* and *-10* were reported in a related species, the marine medaka (Kim *et al*., 2014). In one other species, the Black porgy, *Acanthopagrus schlegeli*, *aqp1a* mRNA levels were reported to be higher in FW than in SW (An *et al*., 2008).

There is not much known about drinking behavior of the adult Japanese medaka or related species. Only a single study reported drinking dynamics, and found that even though more water was imbibed in 80% SW larvae than in FW, there was a significant drinking activity also in FW individuals (Kaneko and Hasegawa, 1999). When inspected upon dissection, we saw unequivocal evidence of drinking in adult medaka in SW. Yellow-whitish precipitates, presumably made of Ca^{2+}- and Mg^{2+}-carbonates (Grosell, 2011), appeared already 24 hours after SW-transfer in support of water absorption and bicarbonate secretion. Very little fluid appeared in the lumen of FW intestines. Na^+,K^+-ATPase α-subunit transcripts were unaffected by salinity, contrasting several other reports of higher Na^+,K^+-ATPase expression and activity in the intestine of SW-teleosts (Grosell, 2011); however, the marked increase in the NKCC2 transcript level in SW, suggests that increased salt transport is indeed taking place, and may be linked to increased water absorption. On the other hand, the decreasing aquaporin level contradicts increased transcellular water transport, and it is therefore puzzling at this moment, how water absorption takes place across the intestinal barrier in the medaka. One possibility is that paracellular water transport may exceed transcellular water transport. This would require a rearrangement of the tight junction apparatus with its associated junctional proteins, and opens an interesting area for future research. To this end claudin-2 has been suggested to create a water pore, since it increases water permeability when over-expressed in MCDK C7 epithelial monolayers (Rosenthal *et al*., 2010). The increased level of NKCC2 may then benefit apical Na^+ uptake directed for secretion into the lateral intercellular space.

Only a few studies have enlightened the molecular pathways for water transport across the teleost intestine. Recent evidence showed that transcellular water transport is predominating in SW-acclimated salmonids (Sundell and Sundh, 2011), as the paracellular permeability of the intestine is

reduced upon SW-acclimation together with an increased transepithelial electrical resistance (TER). Transcellular water absorption was further supported by a recent study of polyethyleneglycol (PEG) permeability in the killifish intestine (Wood and Grosell, 2012). On the contrary, we did not find evidence of an alteration in TER of the intestine related to salinity. The resistance was generally low compared to other investigations (Grosell *et al*., 2009; Sundell and Sundh, 2011), which suggests that the paracellular permeability is quite high in both FW and SW, and supports a paracellular transport route. The study gives rise to the intriguing question why such redundant abundance of three aquaporin paralogs is present in FW medaka intestines - all of which are predominantly expressed in the apical brush border? Aqp1a is a true water pore, Aqp10a presumably has additional permeability to glycerol, whereas the permeability properties of medaka Aqp8ab are unknown at present but may include urea and glycerol as shown in salmon (Engelund *et al*., 2013). Thus at least Aqp8ab and -10a may be involved in metabolism of glycerol and other small solutes linked to digestive processes. A nearby speculation based on our data is that FW medakas absorb significant amounts of water in their intestine, which appears contradictory to the general consensus regarding hyperosmoregulatory mechanisms in teleosts. Feeding fish may swallow water in association with food intake but the fate of any imbibed water has not been studied in detail. Furthermore, fish in our study were non-fed, and drinking seems not to be beneficial for osmoregulatory purposes. A final speculation is that aquaporins may be involved in fluid secretion in the FW medaka intestine. There is no functional evidence to support this at present but this has been shown to occur in FW stickleback males during their sexual maturation when kidney function becomes compromised (De Ruiter, 1980) and in SW killifish intestines, when intracellular cAMP and Ca^{2+} levels are stimulated *in vitro* (Marshall et al., 2002). Irrespective of direction of transport, basolateral expression of aquaporins still needs to be demonstrated for transcellular water transport to take place.

Concluding remarks

This study identified several aquaporin paralogs in Japanese medaka that respond to a changing osmotic environment in different tissues. Most pronounced changes occurred in the skin and gill (*aqp3a*) and in the intestine (*aqp1a, -8ab* and *-10a*), where the levels were much higher in FW than SW, the latter three being at both transcript and protein levels. No changes occurred in Na^+,K^+-ATPase α-subunit expression in the intestine, which is surprising considering its role as a driving force for generation of osmotic gradients across the intestinal epithelium. On the other hand the

absorptive-type NKCC2 cotransporter was much elevated in the SW-intestine, suggesting an increased apical salt absorptive capacity, when drinking is initiated. The study leaves an open question about the molecular pathway for transepithelial water absorption in the SW Japanese medaka intestine. The reduced intestinal aquaporin expression was opposite to our hypothesis, which was based on the assumption that intestinal water absorption was higher in a hyperosmotic medium. An alternative model for intestinal water transport must therefore be proposed in the medaka, with emphasis on the paracellular route compared to other fishes investigated to date, and efforts should be made to analyse the permeability and water transport characteristics of the medaka intestine.

Materials and Methods

Fish and maintenance

Adult Japanese medaka (*Oryzias latipes*, Temminck & Schlegel) were purchased from Aquatic Research Organism (Hampton, NH) and acclimated to experimental conditions in recirculated dechlorinated tap water (FW) or artificial 28 ppt seawater (Instant Ocean, United Pet Group, Blacksburg, VA) at 20 ºC for at least 1 month prior to experiments. They were fed 3 times/day with a mixed diet of Tetramin tropical flakes (Tetra, United Pet group, Blacksburg, VA) and frozen brine shrimp (Bay Brand, San Francisco, Newark, CA) except during the short-term salinity transfer experiments, where food was withheld from one day before and throughout the experiment (3 days). All handling and experimental procedures were approved by the Animal Care and Use Committee of the University of Arkansas (IACUC protocol number 11005).

Experimental setup and sampling

Two experiments were performed: long-term acclimation to FW and SW and short-term transfer from FW to SW and from SW to FW. In the long-term acclimation experiment, 4 fish (2 males and 2 females) were acclimated to FW and 4 fish to 28 ppt SW for at least 1 month. The fish were anaesthetized in 100 mg/L tricaine methanesulfonate (MS-222, buffered with $NaHCO_3$) and then killed by cervical dislocation prior to sampling of gill filaments, intestine, kidney, liver, spleen, gonads, brain, skin, and caudal muscle. Medakas do not have a stomach (Iwamatsu, 2012), so the entire intestine after the esophagus until the anus was used with fat trimmed off. All tissues were immediately frozen on dry ice and stored at -80 ºC until used.

In the short-term time course experiments, medaka (long-term acclimated) were directly transferred from FW to SW or from SW to FW and then sampled (N=10) after 24 and 72 hours. Parallel groups were sham-transferred to the original medium and sampled as controls. Prior to sampling, fish were anaesthetized and killed as described above. The entire caudal peduncle was removed, gently blotted dry with Kimwipes and the wet weight determined. Dry weight and muscle water content (%) were determined after drying overnight at 105 ºC. The entire intestine was dissected as above quickly frozen in dry ice.

RNA isolation, cDNA synthesis and real-time qPCR

Tissues were homogenized in TRI reagent (Sigma-Aldrich, St. Louis, MO) using a rotating knife homogenizer, and total RNA was extracted following the manufacturer's protocol. The RNA pellet was dissolved in nuclease free water and the quantity and purity (A_{260}/A_{280}) were estimated using a NanoDrop spectrophotometer (Thermo Fisher Scientific, Waltham, MA). A_{260}/A_{280} was generally >1.90. First strand cDNA synthesis from 1 µg total RNA was performed in a total volume of 20 µL using Applied Biosystems high capacity cDNA reverse transcription kit (Foster City, CA). Messenger RNA sequences of the following Japanese medaka target transcripts were identified in the Ensemble genome browser (www.ensembl.org/) and used for primer generation (see Table 2): *aqp1a, aqp3a, aqp7, aqp8ab, aqp10a, aqp10b, aqp11a*, Na^+,K^+,$2Cl^-$-cotransporter type 2 (NKCC2), Na^+,K^+-ATPase-α1a, -α1b, -α1c, -α2, -α3a, -α3b, sodium/glucose cotransporter type-1 (SGLT1). Ribosomal protein P0 (*rplp0*), *β-actin* and elongation factor 1-alpha (*EF1α*) were used for internal normalisation. All primers were generated using Primer3 software (Koressaar *et al.*, 2007; Untergrasser *et al.*, 2012). Real-time quantitative PCR was performed using a BioRad CFX96 platform (BioRad, Hercules, CA) and SYBR® Green JumpStart™ Taq ReadyMix™ (Sigma-Aldrich) in a total volume of 15 µL. Primer concentrations were 150 nM and the thermocycling protocol consisted of 3 min initial denaturation (94 ºC), 40-cycles of denaturation (15 s) + annealing/elongation (1 min, 60 ºC), followed by dissociation curve analysis (5 s/ºC, 65-94 ºC). PCR amplification efficiency (84-120%) was analyzed over a 2^8 dilution range and the relative copy numbers were calculated according to Pfaffl (2001) as: $C_n = (1+E_a)^{-Ct}$, where C_n is the relative copy number and C_t is the threshold cycle of the target gene. Corrected expression data for the three normalisation genes were entered into the geNorm software (Biogazelle, Zwijnaarde, Belgium) and a geometric mean was calculated and used for normalisation of all expression data. Contamination of RNA samples with genomic DNA was checked by running qPCR on randomized, diluted RNA

samples ('no amplification control'). Amplification in these samples was $<2^{-8}$ of the corresponding cDNA sample. Primer-dimer association was checked in 'no template controls' without addition of cDNA. The molecular size of all amplicons was verified by 2.5% agarose gel electrophoresis.

Primary antibodies

Based on the Ensembl protein sequences of Japanese medaka Aqp1a, -8ab and -10a, we selected appropriate epitopes for homologous antibody production: Aqp1a: GPVGDYDVNGGNES (c-terminal, amino acid 240-253); Aqp8ab: VDSALMEKGKKPAAC (n-terminal, amino acid 15-28); Aqp10a: CLDEKRNTPAPPDL (cytosol loop, amino acid 170-183). Affinity purified polyclonal antibodies were produced in rabbits by GenScript (Piscataway, NJ), validated by Western blotting and used for immunofluorescence. To detect Na^+,K^+-ATPase we used a monoclonal mouse antibody recognizing all isoforms of the Na^+,K^+-ATPase α-subunit (α5; The Developmental Studies Hybridoma Bank developed under auspices of the NICHD and maintained by The University of Iowa, Department of Biological Sciences, Iowa city, IA). A mouse monoclonal anti-β-actin antibody was used as loading control (mAbcam 8224; ABCAM, Cambridge, MA).

Western blotting

Western blotting was performed as described previously (Tipsmark *et al.*, 2010a). Intestines from FW- and SW-acclimated medaka were homogenized in SEID buffer (mmol L^{-1}: sucrose 300 , Na_2-EDTA 20, imidazole 50, 0.1% sodium deoxycholate, with a protease inhibitor cocktail (P8340; Sigma-Aldrich) centrifuged at 5,000x g for 10 minutes at 4°C. The supernatant was transferred to a new tube and centrifuged at 20,000x g for 1 hour at 4°C. The pellet (membrane fraction) was redissolved in 20µL of SEID buffer. Protein concentration was evaluated using the Bradford assay. Samples were mixed with NuPage LDS sample buffer (Life Technologies, Carlsbad, CA) and added dithiothreitol (50 mmol L^{-1}). Samples were heated at 75°C for 10 minutes. Ten µg of protein was loaded in all lanes and separated in 4–12% bis-Tris gels and MES/SDS buffer at 200 V (Xcell II SureLock, Life Technologies). Molecular sizes were estimated by a Novex sharp Pre-Stained Protein Standard marker (Invitrogen). Following electrophoresis, proteins were electroblotted onto nitrocellulose membranes (0.20 µm; Invitrogen) by submerged blotting for 1 h at 30 V (XCell II; Invitrogen) with transfer buffer (in mmol L^{-1}: 25 Tris, 192 glycin, and 20% methanol). Membranes were blocked in 5% non-fat milk in 1xTBST (in mmol L^{-1}: 50 Tris-Cl, 150 NaCl, 0.1% Tween20, pH 7.5) for 1 hour at 4°C. After blocking, membranes were incubated overnight at 4°C with a cocktail of two primary antibodies (rabbit anti-Aqp1a 0.24 µg mL^{-1}; or anti-Aqp8ab 0.51 µg mL^{-1};

or anti-Aqp10a 0.68 μg mL^{-1}; and mouse anti-β-actin 0.12 μg mL^{-1}). Following 4x5 min washes in 1xTBST buffer, membranes were incubated with IRDye 800-labeled goat-anti rabbit and IRDye 680-labeled mouse antibodies (LiCor Biosciences, Lincoln, NE) diluted 1:10000, for 45 minutes at room temperature. Following 4x5 min final washes in 1xTBST, membranes were air dried and scanned on an infrared imager (Odyssey, Li-Cor Biosciences, Lincoln, NE). The aquaporin band intensities were quantified using the Image Studio Ver. 2.0 software (LiCor Biosciences) and normalized to β-actin. In separate experiments, the ability of the antigenic peptides to neutralize the target protein was validated by pre-incubating the primary antibody with the antigenic peptide in a 400x molar excess overnight at 4°C prior to probing the membrane.

Immunofluorescense microscopy

Intestines from FW and SW-acclimated medaka were fixed overnight in 4% phosphate-buffered paraformaldehyde (4°C). Following several rinses in phosphate buffered saline (PBS; in mmol L^{-1}: 137 NaCl, 2.7 KCl, 4.3 Na_2HPO_4, 1.4 KH_2PO_4, pH 7.3) trimmed sub-samples were then infused in Optimal Cutting Temperature embedding medium (OCT, Sakura® Finetek, AJ Torrance, CA) overnight at 4°C, frozen in cryo-molds on dry ice and stored at -20°C until sectioned. Cryosections (8-10 μm) were prepared on a cryostat HM 525 (Microm International, Walldorf, Germany), transferred to SuperFrost® Plus microslides and dried at 50°C for 3-4 hours before further use. Immunostaining was accomplished by the following protocol: 2x5 min washing in PBS; epitope retrieval by boiling in citrate buffer (10 mmol L^{-1} $Na_3C_6H_5O_7$, pH 6) for 2x5 min, rinsing 5 min in PBS, blocking in 3% normal goat serum/1% bovine serum albumin in PBS for 1 h and incubation in a cocktail of two primary antibodies (rabbit anti-Aqp1a, -8ab, -10a at 1-5 μg $mL^{-1}$and mouse anti-Na^+,K^+-ATPase α-subunit (α5) 0.5 μg mL^{-1}) in blocking buffer overnight (4°C). The next day the sections were washed 3x5 min in PBS and incubated for 1-2 h at 37°C with secondary antibodies (Alexa Fluor 647 conjugated goat-anti rabbit; Oregon green 488 conjugated goat-anti mouse; Life Technologies). Following washes (3x5 min in PBS, 1x5 min in distilled water) the sections were mounted with coverslips using Vectashield mounting medium with 4',6-diamidino-2-phenylindole antifade agent (Vector Laboratories, Burlingame, CA) and examined with a Zeiss Axio Imager M2 microscope (Zeiss, Oberkochen, Germany); pictures were taken with an AxioCam MR monochrome camera and processed using the Axio Vision 4 software (Zeiss).

Electrophysiology

The electrophysiological properties of the intestine were investigated by voltage clamping in an Ussing chamber (Physiological Instruments, San Diego, CA) with identical Ringers' solution on the serosal and mucosal side (in mmol L^{-1}: 140 NaCl, 10 $NaHCO_3$, 4 KCl, 2 NaH_2PO_4, 1 $MgSO_4$, 1 $CaCl_2$, 5.5 glucose, pH 7.8). Fish (N=4) acclimated to FW and 28 ppt SW were anaesthetized in MS-222 and killed by cervical dislocation. The intestine was dissected, fat trimmed away, rinsed in cold PBS and split into anterior (AI, 2/3) and posterior (PI, 1/3) segments based on visual appearance. Each segment was cut into appropriate sections to fit the Ussing chamber slider with an aperture of 0.8 mm^2. In most cases, the AI gave 3 and the PI 1-2 useful sections per fish. The tissues were then stored in cold Ringer's until analyzed. The voltage/current (V/I) relationship was measured immediately after mounting and then again after 5-10 min by clamping the tissue to alternating DC voltages (0, ±0.5, ±1.0, ±1.5 and ±2.0 mV) and measuring the clamp current (Sundell and Sundh, 2011). It took 30-40 min to examine all segments in one fish. The transepithelial resistance (TER, $\Omega*cm^2$) was calculated as the slope of the linear regression line of the V/I relationship.

Statistics

Tissue expression data were analyzed by two-way ANOVA. When required, logarithmic transformation of data was done to meet the ANOVA assumption of homogeneity of variances as tested by Bartlett's test. When the interaction between factors was significant this was followed by Tukey's post-hoc analysis and otherwise the overall effects are indicated in the figures. A significance level of $P<0.05$ was chosen. All tests were performed using GraphPad Prism 5.0 software (San Diego, CA, USA).

Competing interests

The authors declare no competing financial interests.

Author contributions

S.S.M. and C.K.T. conceived and designed the experiments. S.S.M performed the experiments and analyzed the data. J.B. and C.K.T. did the Western analyses. S.S.M. wrote the paper

Funding

S.S.M. was supported by a grant from the Danish Natural Science Council (09-070689) and by a visiting professor scholarship from the Fulbright Foundation. C.K.T. received support from the National Science Foundation (IBN 12-51616) and the Arkansas Biosciences Institute.

References

Aguenaou H., Boeuf G., and Colin, D.A. (1989). Na^+ uptake through the brush border membranes of intestine from fresh water and sea-water adapted trout (*Salmo gaidneri*, R.). *J. Comp. Physiol. B: Biochem. Syst. Environ. Physiol.* **159**, 275-280.

Aoki, M., Kaneko, T. Katoh, ., Hasegawa, S., Tsutsui, N. and Aida, K. (2003). Intestinal water absorption through aquaporin 1 expressed in the apical membrane of mucosal epithelial cells in seawater-adapted Japanese eel. *J. Exp. Biol.* **206**, 3495-3505.

An, K.W., Kim, N.N. and Choi, C.Y. (2008). Cloning and expression of aquaporin 1 and arginine vasotocin receptor mRNA from the black porgy, *Acanthopagrus schlegeli*: effect of freshwater acclimation. *Fish Physiol. Biochem.* **34**, 185-194.

Brunelli, E., Mauceri, A., Salvatore, F., Giannetto, A., Maisano, M. and Tripepia, S. (2010). Localization of aquaporin1 and 3 in the gills of the rainbow wrasse *Coris julis*. *Acta histochem.* **112**, 251-258.

Cerdà, J. and Finn, R.N. (2010). Piscine aquaporins: an overview of recent advances. *J. Exp. Zool.* **313A**, 623-650.

Choi, Y.J., Shin, H.S., Kima, N.N., Cho, S.H., Yamamoto, Y., Ueda, H., Lee, J. and Choi, C.Y. (2013). Expression of aquaporin-3 and −8 mRNAs in the parr and smolt stages of sockeye salmon, *Oncorhynchus nerka*: Effects of cortisol treatment and seawater acclimation. *Comp. Biochem. Physiol.* **165A**, 228-236.

Cutler, C. and Cramb, G. (2002). Branchial expression of an aquaporin 3 (AQP-3) homologue is downregulated in the European eel *Anguilla anguilla* following seawater acclimation. *J. Exp. Biol.* **205**, 2643-2651.

Deane, E.E. and Woo, N.Y.S. (2006). Tissue distribution, effects of salinity acclimation, and ontogeny of aquaporin 3 in the marine teleost, Silver Sea Bream (*Sparus sarba*). *Marine Biotech.* **8**, 663-671.

De Ruiter A.J.H. (1980) Effects of testosterone on kidney structure and hydromineral regulation in the teleost *Gasterosteus aculeatus* L. Dissertation, State University of Groningen, The Netherlands.

Diamond, J.M. and Bossert, W.H. (1967). Standing gradient osmotic flow. A mechanism for coupling of water and solute transport in epithelia. *J. Gen. Physiol.* **50**, 2061–2083.

Elkjær, M.L., Nejsum, L.N., Gresz, V., Kwon, T.-H., Jensen, U.B., Frøkiær, J. and Nielsen, S. (2001). Immunolocalization of aquaporin-8 in rat kidney, gastrointestinal tract, testis, and airways. *Am. J. Physiol.* (*Renal. Physiol.*) **281**, 1047-1057.

Engelund, M.B., Chauvigné, F., Christensen, B.M., Finn, R.N., Cerdà, J. and Madsen, S.S. (2013). Differential expression and novel permeability properties of three quaporin 8 paralogs from seawater-challenged Atlantic salmon smolts. *J. Exp. Biol.* **216**, 3873-3885.

Evans, D.H., Piermarini, P.M. and Choe, K.P. (2005). The multifunctional fish gill: Dominant site of gas exchange, osmoregulation, acid-base regulation, and excretion of nitrogenous waste. *Physiol. Rev.* **85**, 97–177.

Fabra, M., Raldúa, D., Power, D.M., Deen, P.M.T. and Cerdà, J. (2005). Marine fish egg hydration is aquaporin-mediated. *Science* **307**, 545.

Giffard-Mena, I., Boulo, V., Aujoulat, F, Fowden, H., Castille, R., Charmantier, G. and Cramb, G. (2007). Aquaporin molecular characterization in the sea-bass (*Dicentrachus labrax*): the effect of salinity on AQP1 and AQP3 expression. *Comp. Biochem. Physiol.* **148A**, 430-444.

Giffard-Mena, I., Lorin-Nebel, C., Charmantier, G., Castille, R. and Boulo, V. (2008). Adaptation of the sea-bass (*Dicentrarchus labrax*) to fresh water: Role of aquaporins and Na^+/K^+-ATPases. *Comp. Biochem. Physiol.* **150A**, 332–338.

Grosell, M. (2011). Intestinal anion exchange in marine teleosts is involved in osmoregulation and contributes to the oceanic inorganic carbon cycle. *Acta Physiol.* **202**, 421-434.

Grosell, M. Genz, J., Taylor, J.R., Perry, S.F. and Gilmour K.K. (2009). The involvement of H^+-ATPase and carbonic anhydrase in intestinal HCO_3^- secretion in seawater-acclimated rainbow trout. *J. Exp. Biol.* **212**, 1940-1948.

Hamann, S., Herrera-Perez, J.J., Bundgaard, M., Leefmans, F.J. and Zeuthen, T. (2005). Water permeability of Na^+-K^+-$2Cl^-$ cotransporters in mammalian epithelial cells. *J. Physiol. London* **568**, 123-135.

Hara-Chikuma, M. and Verkman, A.S. (2006). Physiological roles of glycerol-transporting aquaporins: the aquaglyceroporins. *Cell. Mol. Life Sci.* **63**, 1386-1392.

649 **Hatakeyama, S., Yoshida, Y., Tani, T., Koyama, Y., Nihei, K., Ohshiro, K., Kamiie, J.-I.,**
650 **Yaoita, E., Suda, T., Hatakeyama, K. and Yamamoto, T.** (2001). Cloning of a new aquaporin
651 (AQP10) abundantly expressed in duodenum and jejunum. *Biochem. Biophys. Res. Commun.*
652 **287,** 814-819.
653 **Hendriks, G., Koudijs, M., van Balkom, B.W.M., Oorschot, V., Klumperman, J., Deen, P.M.T**
654 **and van der Sluijs, P.** (2004). Glycosylation is important for cell surface expression of the
655 water channel aquaporin-2 but is not essential for tetramerization in the endoplasmic reticulum.
656 *J. Biol. Chem.* **279**, 2975–2983.
657 **Hwang, P.P., Lee, T. and Lin, I.** (2011). Ion regulation in fish gills: recent progress in the cellular
658 and molecular mechanisms. *Am. J. Physiol. (Regul. Integr. Comp. Physiol.)* **301**, R28–R47.
659 **Isenring, P., Jacoby, S.C., Payne, J.A. and Forbush III, B.** (1998). Comparison of Na-K-Cl
660 cotransporters. NKCC1, NKCC2, and the HEK cell Na-K-Cl cotransporter. *J. Biol. Chem.* **273**,
661 11295-11301.
662 **Ikeda, M., Ando, A., Shimono, M., Takamatsu, N., Taki, A., Muta, K., Matsushita, W., Uechi,**
663 **T., Matsuzaki, T., Kenmochi, N., Takata, K., Sasaki, S., Ito, K. and Ishibashi, K.** (2011).
664 The NPC motif of aquaporin-11, unlike the NPA motif of known aquaporins, is essential for full
665 expression of molecular function. *J. Biol. Chem.* **286**, 3342-3350.
666 **Inoue, K. and Takei, Y.** (2003). Asian medaka fishes offer new models for studying mechanisms
667 of seawater adaptation. *Comp. Biochem. Physiol.* **136B**, 635–645.
668 **Ishikawa, Y.** (2000). Medakafish as a model system for vertebrate developmental genetics.
669 *BioEssays* **22**, 487–495.
670 **Ishibashi, K., Hara, S. and Kondo, S.** (2009). Aquaporin water channels in mammals. *Clin. Exp.*
671 *Nephrol.* **13**, 107-117.
672 **Ishibashi, K., Imaia, M. and Sasaki, S.** (2000a). Cellular localization of aquaporin 7 in the rat
673 kidney. *Exp. Nephrol.* **8**, 252-257.
674 **Ishibashi, K., Kuwahara, M., Kageyama, Y., Sasaki, S., Suzuki, M. and Imai, M**. (2000b).
675 Molecular cloning of a new aquaporin superfamily in mammals: AQPX1 and AQPX2. In:
676 *Molecular biology and physiology of water and solute transport* (ed. S. Hohmann and S.
677 Nielsen), pp. 123-126. New York: Kluwer Academic/Plenum Publishers.
678 **Ishibashi, K., Morinaga, T., Kuwahara, M., Sasaki, S. and Imai, M.** (2002). Cloning and
679 identification of a new member of water channel (AQP10) as an aquaglyceroporin. *Biochim.*
680 *Biophys. Acta* **157**, 335- 340.

Iwamatsu, T. (2012). Growth of the Medaka (I) - Formation of vertebrae, changes in blood circulation, and changes in digestive organs. *Bull. Aichi Univ. Education (Natural Sciences)* **61**, 55-63.

Jung, D., Sato, J.D., Shaw, J.R. and Stanton, B.A. (2012). Expression of aquaporin 3 in gills of the Atlantic killifish (*Fundulus heteroclitus*): Effects of seawater acclimation. *Comp. Biochem. Physiol.* **161A**, 320-326.

Kaneko, T. and Hasegawa, S. (1999). Application of laser scanning microscopy to morphological observations on drinking in freshwater medaka larvae and those exposed to 80% seawater. *Fisheries Sci*. **65**, 492-493.

Kang, C.-K., Tsai, H.-J., Liu, C.-C., Lee, T.-H. and Hwang, P.-P. (2010) Salinity-dependent expression of a Na^+, K^+, $2Cl^-$- cotransporter in gills of the brackish medaka *Oryzias dancena*: A molecular correlate for hyposmoregulatory endurance. *Comp. Biochem. Physiol.* **157A**, 7-18.

Kang, C.-K., Tsai, S.-C., Lee, T.-H. and Hwang, P.P. (2008). Differential expression of branchial Na^+/K^+-ATPase of two medaka species, *Oryzias latipes* and *Oryzias dancena*, with different salinity tolerances acclimated to fresh water, brackish water and seawater. *Comp. Biochem. Physiol.* **151A**, 566–575.

Kim, Y.K., Lee, S.Y., Kim, B.S., Kim, D.S., Nam, Y.K. (2014). Isolation and mRNA expression analysis of aquaporin isoforms in marine medaka *Oryzias dancena*, a euryhaline teleost. *Comp. Biochem. Physiol.* **171A,** 1–8.

Kim, Y.K., Watanabe, S., Kaneko, T., Huh, M.D. and Park, S.I. (2010). Expression of aquaporins 3, 8 and 10 in the intestines of freshwater- and seawater-acclimated Japanese eels *Anguilla japonica*. *Fisheries Sci.* **76**, 695-702.

Kim, Y.K., Watanabe, S., Park, S.I., Jeong, J.B., Kaneko, T., Park, M.A. and Yeo, I.K. (2013). Molecular characterization and gene expression of Na^+-K^+-$2Cl^-$- cotransporter2 (NKCC2) in the gastrointestinal tract of Olive flounder (*Paralichythys olivaceus*) during the four days after infection with *Streptococcus parauberis*. *Mar. Fresh. Behav. Physiol.* **46**, 145-157.

King, L.S., Kozono, D. and Agre, P. (2004). From structure to disease: the evolving tale of aquaporin biology. *Nature Reviews Mol. Cell Biol.* **5**, 687-698.

Koressaar, T. and Remm, M. (2007). Enhancements and modifications of primer design program Primer3. *Bioinformatics* **23**, 1289-1291.

Krogh, A. (1937). Osmotic regulation in freshwater fishes by active absorption of chloride ions. *Z. Vgl. Physiol.* **24**, 656-666.

Laforenza, U., Cova, E., Gastaldi, G., Tritto, S., Grazioli, M., LaRusso, N.F., Splinter, P.L., D'Adamo, P., Tosco, M. and Ventura, U. (2005). Aquaporin-8 is involved in water transport in isolated superficial colonocytes from rat proximal colon. *J. Nutr.* **135**, 2329-2336.

Laforenza, U., Scaffino, M.F. and Gastaldi, G. (2013). Aquaporin-10 represents an alternative pathway for glycerol efflux from human adipocytes. *PLOS One* **8**, e54474.

Larsen, E.H. and Møbjerg, N. (2006). Na^+ recirculation and isosmotic transport. *J. Membrane Biol.* **212**, 1–15.

Li, H., Kamiie, J., Morishita, Y., Yoshida, Y., Yaoita, E., Ishibashi, E. and Yamamoto, T. (2005). Expression and localization of two isoforms of AQP10 in human small intestine. *Biol. Cell* **97**, 823-829.

Lignot, J.-H., Cutler, C.P., Hazon, N. and Cramb, G. (2002). Immunolocalisation of aquaporin 3 in the gill and the gastrointestinal tract of the European eel *Anguilla anguilla* (L.). *J. Exp. Biol.* **205**, 2653-2663.

Loo, D.D.F., Hirayama, B.A., Meinild, A.-K., Chandy, G., Zeuthen, T. and Wright, E.M. (1999). Passive water and ion transport by cotransporters. *J. Physiol.* **518**, 195-202.

Loo, D.D.F., Wright, E.M. and Zeuthen, T. (2002). Water pumps. *J. Physiol*. **542**, 53–60.

Loo, D.D.F., Zeuthen, T., Chandy, G. and Wright, E.M. (1996). Cotransport of water by the Na^+/glucose cotransporter. *Proc. Natl. Acad. Sci. USA* **93**, 13367-13370.

Lytle C., Xu, J.C., Biemesderfer, D. and Forbush, B. (1995). Distribution and diversity of Na-K-Cl cotransporter proteins: a study with monoclonal antibodies. *Am. J. Physiol. (Cell Physiol.)* **269**, C1469-C1505.

MacIver, B., Cutler, C.P., Yin, J., Hill, M.G., Zeidel, M.L. and Hill, W.G. (2010). Expression and functional characterization of four aquaporin water channels from the European eel (*Anguilla anguilla*) *J. Exp. Biol.* **212**, 2856-2863.

Madsen, S.S., Olesen, J.H., Bedal, K., Engelund, M.B., Velsaco-Santamaria, Y.M. and Tipsmark, C.K. (2011). Functional characterization of water transport and cellular localization of three aquaporin paralogs in the salmonid intestine. *Frontiers in Aquatic Physiology* doi: 10.3389/fphys.2011.00056.

Marshall, W.S., Howard, J.A., Cozzi R.R.F. and Lynch, E.M. (2002). NaCl and fluid secretion by the intestine of the teleost *Fundulus heteroclitus*: involvement of CFTR, *J. Exp. Biol.* **205**, 745–758.**Martinez, A.-S., Cutler, C.P., Wilson, G.D., Phillips, C., Hazon, N. and Cramb, G.** (2005). Regulation of expression of two aquaporin homologs in the intestine of the European eel:

effects of seawater acclimation and cortisol treatment. *Am. J. Physiol.* (*Regul. Integr. Comp. Physiol.*) **288**, R1733-R1743.

Mobasheri, A. and Marples, D. (2004). Expression of the AQP-1 water channel in normal human tissues: a semiquantitative study using tissue microarray technology. *Am. J. Physiol. (Cell Physiol.*) **286**, C529-C537.

Mobasheri, A., Shakibaei, M. and Marples, D. (2004). Immunohistochemical localization of aquaporin 10 in the apical membranes of the human ileum: a potential pathway for luminal water and small solute absorption. *Histochem. Cell Biol.* **121**, 463-471.

Morinaga, T., Nakakoshi, M., Hirao, A., Imai, M. and Ishibashi, K. 2002. Mouse aquaporin 10 gene (AQP10) is a pseudogene. *Biochem. Biophys. Res. Commun.* **294**, 630-634.

Morishita, Y., Matsuzaki, T., Hara-chikuma, M., Andoo, A., Shimono, M., Matsuki, A., Kobayashi, K., Ikeda, M., Yamamoto, T., Verkman, A., Kusano, E., Ookawara, S., Takata, K., Sasaki, S. and Ishibashi, K. (2005). Disruption of aquaporin-11 produces polycystic kidneys following vacuolization of the proximal tubule. *Mol. Cell. Biol.* **25**, 7770-7779.

O'Grady, S.M., Musch, M.W. and Field, M. (1986). Stoichiometry and ion affinities of the Na-K-Cl cotransport system in the intestine of the winter flounder (*Pseudopleurouectes americanus*). *J. Membr. Biol.* **91**, 33-41.

Pandey, R.N., Yaganti, S., Coffey, S., Frisbie, J., Alnajjar, K. and Goldstein, D. (2010). Expression and immunolocalization of aquaporins HC-1, -2, and -3 in Cope's gray treefrog, *Hyla chrysoscelis*. *Comp. Biochem. Physiol.* **157**, 86–94.

Pfaffl, M.W. (2001). A new mathematical model for relative quantification in real-time RT-PCR. *Nucleic Acids Res*. **29**: e45.

Polakof, S., Álvarez, R. and Soengas, J.L. (2010). Gut glucose metabolism in rainbow trout: implications in glucose homeostasis and glucosensing capacity. *Am. J. Physiol.* (*Regul. Integr. Comp. Physiol.*) **299**, R19-R32.

Raldúa, D., Otero, D., Fabra, M. and Cerdà, J. (2008). Differential localization and regulation of two aquaporin-1 homologs in the intestinal epithelia of the marine teleost *Sparus aurata*. *Am. J. Physiol.* (*Regul. Integr. Comp. Physiol.*) **294**, R993–R1003.

Rodríguez A, Catalán V, Gómez-Ambrosi J, García-Navarro S, Rotellar F, Valentí, V., Silva, C., Gil, M.J., Salvador, J., Burrell, M.A., Calamita, G., Malagón, M.M. and Frühbeck, G. (2011). Insulin- and leptin-mediated control of aquaglyceroporins in human adipocytes and

776 hepatocytes is mediated via the PI3K/Akt/mTOR signaling cascade. *J. Clin. Endocrinol. Metab.*
777 **96**, E586-597.
778 **Rosenthal, R., Milatz, S., Krug, S.M., Oelrich, B., Schulzke, J.-D., Amasheh, S., Günzel, D.**
779 **and Fromm, M.** (2010). Claudin-2, a component of the tight junction, forms a paracellular water
780 channel. *J. Cell Sci.* **123**, 1913-1921.
781 **Russell, J.M.** (2000). Sodium-potassium-chloride cotransport. *Physiol Rev* **80**, 211-276.
782 **Sakamoto, T., Kozaka, T., Takahashi, A., Kawauchi, H. and Ando, M.** (2001). Medaka
783 (*Oryzias latipes*) as a model for hypoosmoregulation of euryhaline fishes. *Aquaculture* **193**, 347-
784 354.
785 **Santos, C.R.A., Estêvão, M. D., Fuentes, J., Cardoso, J.C.R., Fabra, M., Passos, A.L.,**
786 **Detmers, F.J., Deen, P.M.T., Cerdà, J. and Power, D.M.** (2004). Isolation of a novel
787 aquaglyceroporin from a marine teleost (*Sparus auratus*): function and tissue distribution. *J. Exp.*
788 *Biol.* **207**, 1217-1227.
789 **Saparov, S. M., Liu, K., Agre, P. and Pohl, P.** (2007). Fast and selective ammonia transport by
790 aquaporin-8. *J. Biol. Chem.* **282**, 5296-5301.
791 **Smith, H.W.** (1929). The excretion of ammonia and urea by the gills of fish. *J. Biol. Chem.* **81**,
792 727–742.
793 **Sundell, K. and Sundh, H.** (2011). Intestinal fluid absorption in anadromous salmonids:
794 Importance of tight junctions and aquaporins. *Frontiers in Aquatic Physiology* doi: 10.3389/
795 fphys.2012.00388.
796 **Tanaka, M.** (1995). Characteristics of medaka genes and their promoter regions. *Fish Biol. J.*
797 *Medaka* **7**, 11–14.
798 **Tingaud-Sequeira, A., Calusinska, M., Finn, R.N., Chauvigné, F., Lozano, J. and Cerdà, J.**
799 (2010). The zebrafish genome encodes the largest vertebrate repertoire of functional aquaporins
800 with dual paralogy and substrate specificities similar to mammals. *BMC Evol. Biol*. 10**,** 38.
801 **Tipsmark, C.K., Mahmmoud, Y.A., Borski, R.J. and Madsen S.S.** (2010a). FXYD-11 associates
802 with Na^+-K^+-ATPase in the gill of Atlantic salmon: regulation and localization in relation to
803 changed ion-regulatory status. *Am. J. Physiol.* **299**, R1212-R1223.
804 **Tipsmark, C.K., Sørensen, K.J. and Madsen, S.S.** (2010b). Aquaporin expression dynamics in
805 osmoregulatory tissues of Atlantic salmon during smoltification and seawater acclimation. *J.*
806 *Exp. Biol.* **213**,368-379.

Tse, W.K.F., Au, D.W.T. and Wong, C.K.C. (2006). Characterization of ion channel and transporter mRNA expressions in isolated gill chloride and pavement cells of seawater acclimating eels. *Biochem. Biophys. Res. Commun.* **346**,1181-1190.

Tyagi, M.G. and Tangevelu, P. (2010). A possible role of aquaporin water channels in blood cell migration in spleen; interaction with cluster of differentiation molecules. *J. Exp. Sci.***1**, 41-42.

Untergrasser A, Cutcutache I, Koressaar T, Ye J, Faircloth BC, Remm M, Rozen SG (2012). Primer3 - new capabilities and interfaces. Nucleic Acids Res. **40**: e115.

Wakayama, Y., Inoue, M., Kojima, H., Jimi, T., Shibuya, S., Hara, H. and Oniki, H. (2004). Expression and localization of aquaporin 7 in normal skeletal myofiber. *Cell. Tissue Res.* **316**, 123-129.

Watanabe, S., Kaneko, T. and Aida, K. (2005). Aquaporin-3 expressed in the basolateral membrane of gill chloride cells in Mozambique tilapia *Oreochromis mossambicus* adapted to freshwater and seawater. *J. Exp. Biol.* **208**, 2673-2682.

Watanabe, S., Mekuchi, M., Ideuchi, H., Kim, Y.K. and Kaneko, T. (2011). Electroneutral cation-Cl^-- cotransporters NKCC2β and NCCβ expressed in the intestinal tract of Japanese eel *Anguilla japonica*. *Comp. Biochem. Physiol.* **159A**, 427-435.

Wood, C.M. and Grosell, M. (2012). Independence of net water flux from paracellular permeability in the intestine of *Fundulus heteroclitus*, a euryhaline teleost. *J. Exp. Biol.* **215**, 508-517.

Yakata, K., Hiroaki, Y., Ishibashi, K., Sohara, E., Sasaki, S., Mitsuoka, K. and Fujiyoshi, Y. (2007). Aquaporin-11 containing a divergent NPA motif has normal water channel activity. *Biochim. Biophys. Acta* **1768**, 688-693.

Xue, H., Liu, S.M., Ji, T., Ren, W., Zhang, X.H., Zheng, L.F., Wood, J.D. and Zhu J.X. (2009). Expression of NKCC2 in the rat gastrointestinal tract. *Neurogastroenterol. Motil.* **21**, 1068-1076.

Figure legends

Fig. 1. Transcript levels of aquaporins (A-G) and the NKCC2 cotransporter (H) in various tissues from Japanese medaka. Bars represent the mean value of 4 FW- and 4 SW-acclimated fish (4 males + 4 females) + s.e.m. Expression levels are shown in arbitrary units as calculated relative to the geometric mean of three normalization (see Methods), and for each transcript subsequently normalized relative to the highest expression level (=100). Shared letters above the bars indicate not significantly different. An asterisk (*) above a bar indicates that FW value was significantly higher than SW value; a cross (#) above a bar indicates that SW value was significantly higher than FW values. $P < 0.05$, Bonferoni adjusted least significant differences test.

Fig. 2. The effect of FW-to-SW transfer on transcript levels of intestinal aquaporins (A-G) and muscle water content (H) of Japanese medaka. Fish were transferred from FW to SW or FW to FW as control at time zero and sampled at 24 and 72 hours (N=6). Expression levels are shown in arbitrary units as calculated relative to the geometric mean of three normalization (see Methods), and for each transcript subsequently normalized to the level of the 24 h FW group. The labels "sal", "time" and "sal x time" refer to overall factorial effects (salinity and time) and their interaction (2-way ANOVA) at the P-level indicated by the number of asterisks: * $P<0.05$, ** $P<0.01$; *** $P<0.001$. In the case of factorial interaction, FW and SW mean values were compared at each time point (Student's t-test) and significance is indicated by a cross (#) above a bar. Values are means + s.e.m.

Fig. 3. The effect of FW-to-SW transfer on transcript levels of Na^+,K^+-ATPase alpha subunit isoforms (A-F), the NKCC2 cotransporter (G) and the sodium-glucose tranporte type-1 (H) in the intestine of Japanese medaka. Fish were transferred from FW to SW or FW to FW as control at time zero and sampled at 24 and 72 hours (N=6). For further explanation see the legend to Fig. 2.

Fig. 4. The effect of SW-to-FW transfer on transcript levels of intestinal aquaporins (A-G) and muscle water content (H) of Japanese medaka. Fish were transferred from SW to FW or SW to SW as control at time zero and sampled at 24 and 72 hours (N=6). For further explanation see the legend to Fig. 2.

Fig. 5. The effect of SW-to-FW transfer on normalized transcript levels of Na^+,K^+-ATPase alpha subunit isoforms (A-F), the NKCC2 cotransporter (G) and the sodium-glucose tranporter type-1 (H) in the intestine of Japanese medaka. Fish were transferred from SW to FW or SW to SW as control at time zero and sampled at 24 and 72 hours (N=6). For further explanation see the legend to Fig. 2.

Fig. 6. Western blots of enriched membrane fractions from homogenized intestines of FW Japanese medaka. Membrane strips were probed with a cocktail of two primary antibodies against one of the three aquaporins: Aqp1a (lane 2), Aqp8ab (lane 6) and Aqp10a (lane 10) (green bands) and β-actin (red band). Lanes 1, 3, 5, 7, 9 and 11 show the molecular weight marker as indicated to the left. The Aqp antibodies recognize major immunoreactive proteins around 25 kDa (Aqp1a), 28 kDa and a duplet around 35-40 kDa (Aqp8ab) and 35 kDa (Aqp10a), respectively. The β-actin antibody recognizes one band around 43 kDa. In lanes 4, 8, and 12 (block) the Aqp antibodies are neutralized by 400x molar excess of the antigenic peptide prior to incubation. Upon neutralization, the Aqp-specific band(s) are weakened or disappear.

Fig. 7. Quantification of Western blots by densitometric scanning. Membrane fractions from intestines of 5 FW- and 5 SW-acclimated Japanese medaka were analyzed by Western blotting using a cocktail of two primary antibodies against one of the three aquaporins (Aqp1a, Aqp8ab, Aqp10a) and β-actin as loading control. The specific bands were quantified by densitometric scanning and normalized to β-actin. Asterisks (*) indicate significant difference from the corresponding FW value, Student's t-test, $P<0.05$. Values are means + s.e.m.

Fig. 8. Representative micrographs of intestinal cross sections from FW (A,B) and SW (C,D) Japanese medaka probed with a cocktail of primary antibodies against Aqp1a (red) and the Na^+,K^+-ATPase alpha subunit (green). Nuclei are stained with DAPI and appear blue. A pronounced apical Aqp staining is lining the FW intestine and disappears or is retracted into the cytosolic compartment in the SW intestine. Bars indicate 50 µm.

Fig. 9. Representative micrographs of intestinal cross sections from FW (A,B,C) and SW (D,E,F) Japanese medaka probed with a cocktail of primary antibodies against Aqp8ab (red) and the Na^+,K^+-ATPase alpha subunit (green). Nuclei are stained with DAPI and appear blue. A

pronounced apical Aqp staining is lining the FW intestine and disappears or is retracted into the cytosolic compartment in the SW intestine. Bars indicate 50 µm.

Fig. 10. Representative micrographs of intestinal cross sections from FW (A,B) and SW (C,D) Japanese medaka probed with a cocktail of primary antibodies against Aqp10a (red) and the Na^+,K^+-ATPase alpha subunit (green). Nuclei are stained with DAPI and appear blue. In (B) only the red and blue channels are shown. A pronounced apical Aqp staining is lining the FW intestine and disappears or is diminished in the SW intestine. Bars indicate 20 or 50 µm as indicated.

Table 1. Transepithelial resistance (TER in Ω*cm^2) in anterior and posterior regions of the intestine of Japanese medaka acclimated to FW and SW.

	Anterior	Posterior
FW	12.2 ± 1.7	3.4± 0.7
SW	9.7 ± 1.9	3.7± 1.5

Each region was examined in triplicate-quadruplicate sections from the same fish (N=4). There was an overall effect of region ($P<0.0005$, 2-way ANOVA) but not salinity on TER.

911 **Table 2: Primer sequences for quantitative real time PCR of Japanese medaka transcript**
912 **targets and normalisation genes.**
913

Target name	Forward primer	Reverse primer	Ensemble ID	Amplicon size (bp)
Aqp1a	CTGGGACATTTGGCAGCTAT	CCAGTGGTCCGTAAAATCGT	ENSORLT00000022053	99
Aqp3a	GCCTTCACTGTGGGATTTGT	GAGGTCTCTGGCAGGATTGA	ENSORLT00000012760	87
Aqp7	GACATTGCACCCAGGTTCTT	CAACTAGAGGCACCCACCAC	ENSORLT00000011131	91
Aqp8ab	GCTGCTAAGCCTCCCAGTAA	CCGACACACAACCAATGAAG	ENSORLT00000003813	97
Aqp10a	CAGGCTGGGGTACAGAAGTC	CCAAAATGCCTCCAAGAAGA	ENSORLT00000012051	84
Aqp10b	GCTGAATGTCTGGGGGTCTA	AATCCCAGGTTGATGGACAG	ENSORLT00000000413	110
Aqp11a	TCGAGAAAATCCTCCCCTTC	ACAGCCTCTTCTGCTTCTGG	ENSORLT00000018867	81
NKCC2	ACCATTGCTCCCATCATCTC	TGGAGACCGAGCATAAGAGG	ENSORLT00000003347	90
SGLT1	AACTGCTGCCGATGTTTCTT	CCGACACCAGAGTCACAGAA	ENSORLT00000012185	118
Atp-α1a	ATCCTCGCCAGTATCCCTCT	TGTCGCTCTCAGCTTCTTCA	ENSORLT00000023207	111
Atp-α1b	GAACCGTCACCATCCTCTGT	TGTCGCTCTCAGCTTCTTCA	ENSORLT00000002643	83
Atp-α1c	CAGCTGGACGACATTTTGAA	CCTGTCTCTGACAGCCCTTCC	ENSORLT00000002556	97
Atp-α2	TTCAGTGGGCGGATCTTATC	CAGAGCCGTCTCAACAAACA	ENSORLT00000003295	107
Atp-α3a	CGTCATCATGGCTGAAAATG	ATTGCTGGCCATAGCTGTCT	ENSORLT00000008844	106
Atp-α3b	TTGCCCCCTTAATGTCACTC	GGGGCAGTTGTGATGAAAAT	ENSORLT00000016540	85
rplp0	AGAGTCCTGGCAGTTGCTGT	AGCAGCAAAAGCAGTTGGAT	ENSORLT00000011509	93
β-actin	GAGAGGGAAATTGTCCGTGA	CTTCTCCAGGGAGGAAGAGG	ENSORLT00000017152	102
EF-1α	ACGTGTCCGTCAAGGAAATC	TGATGACCTGAGCGTTGAAG	ENSORLT00000009544	96

914

915 **Figure 1**

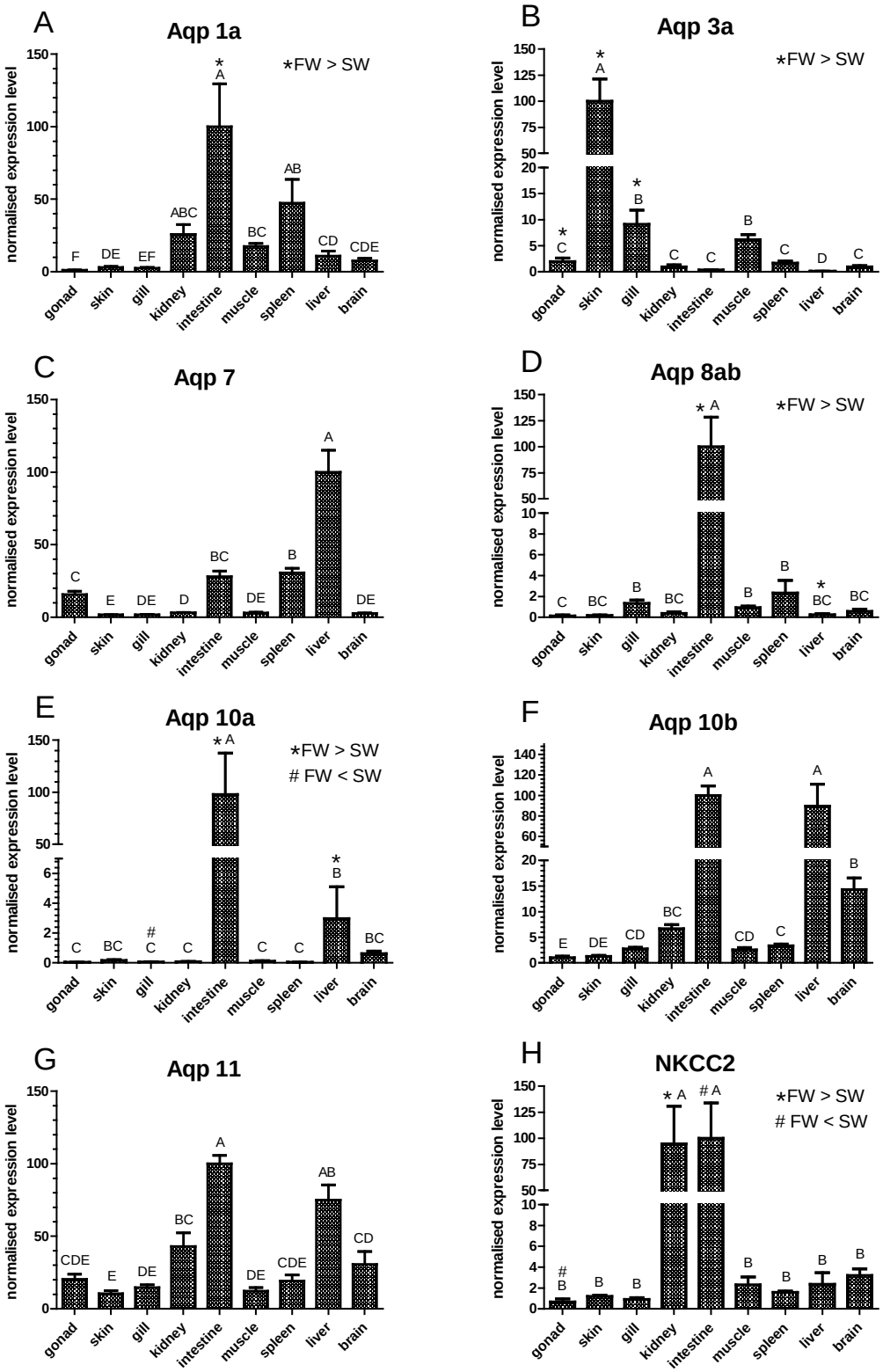

916

917

Figure 2

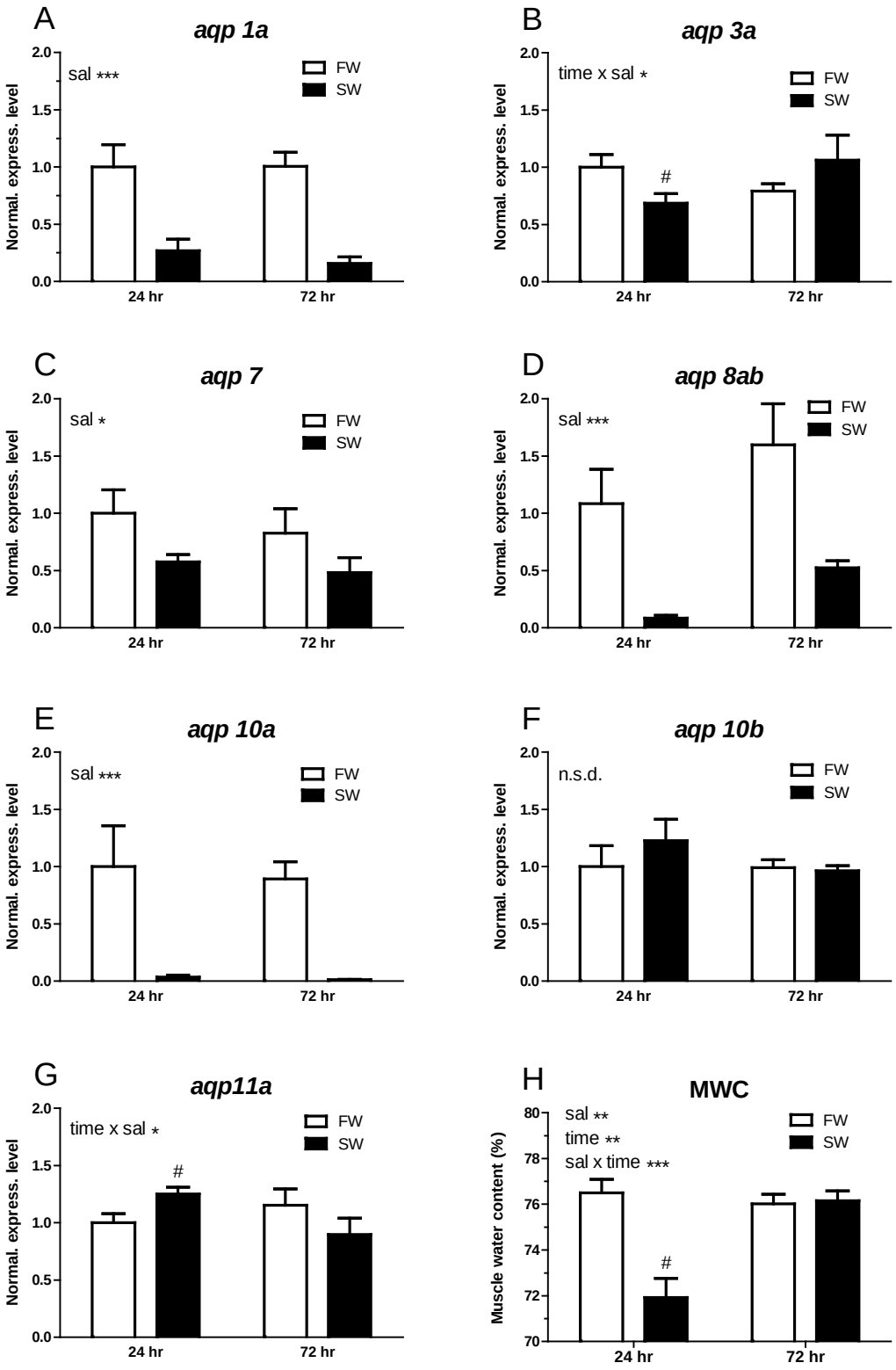

Figure 3

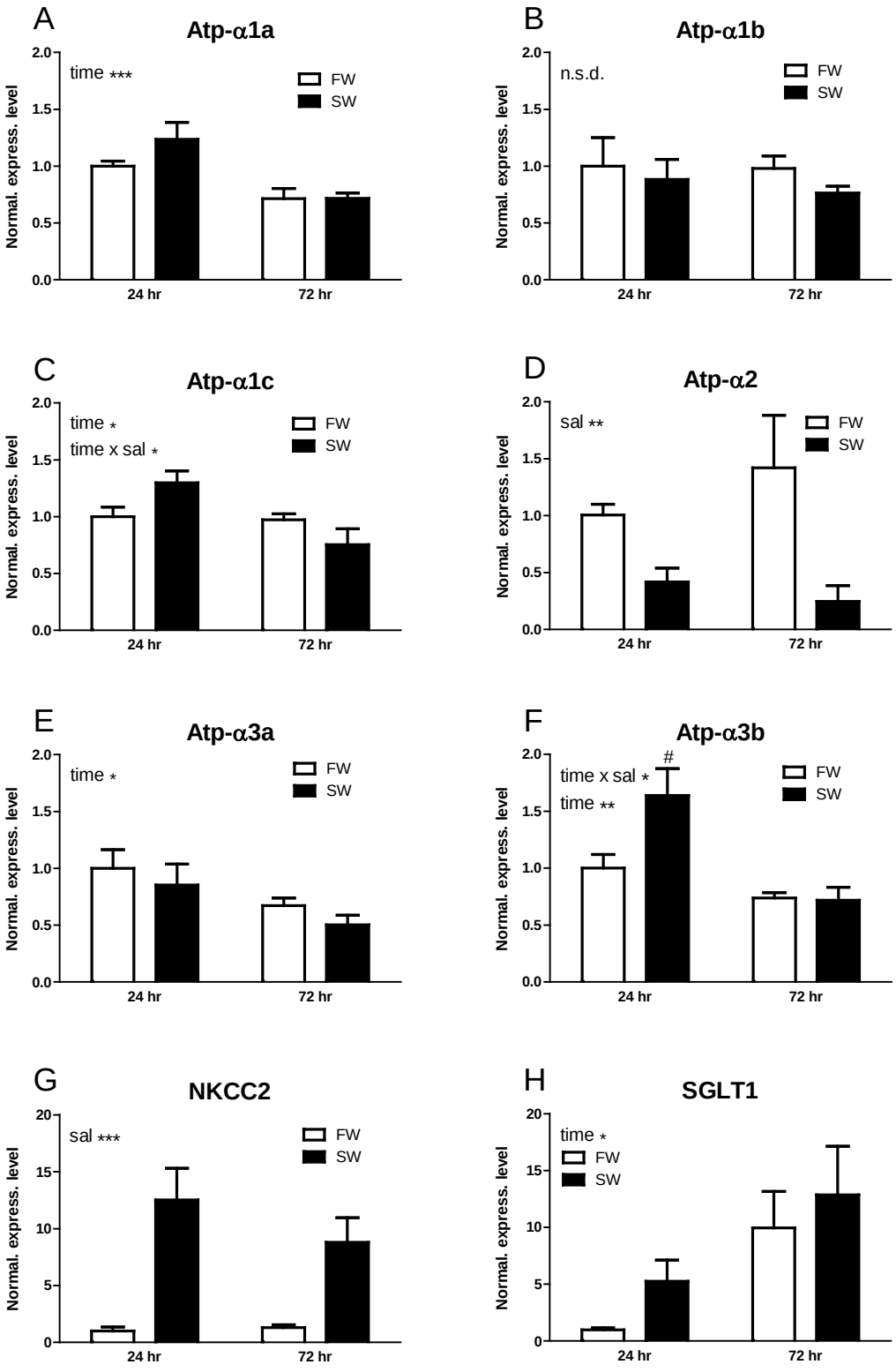

Figure 4

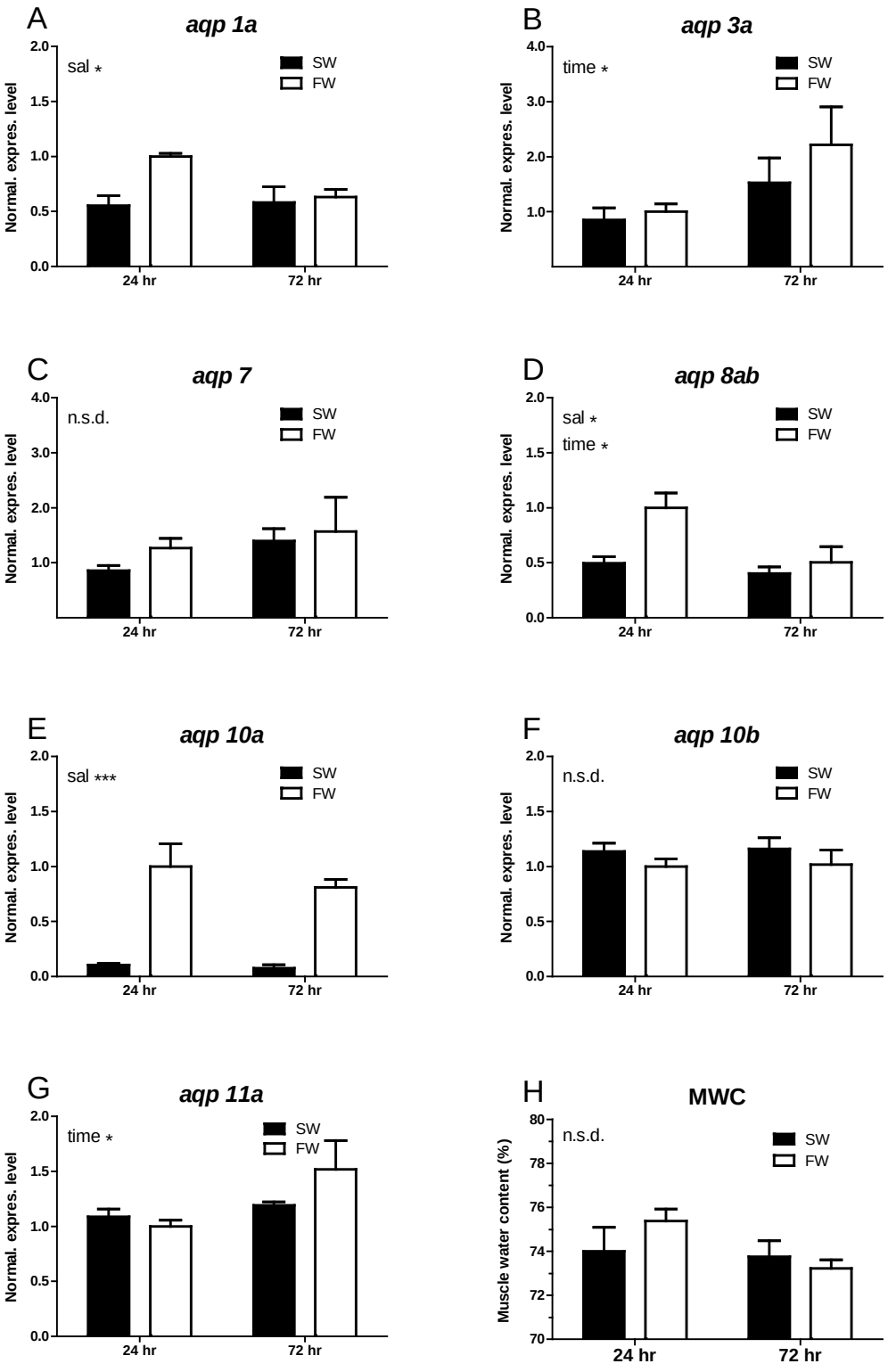

Figure 5

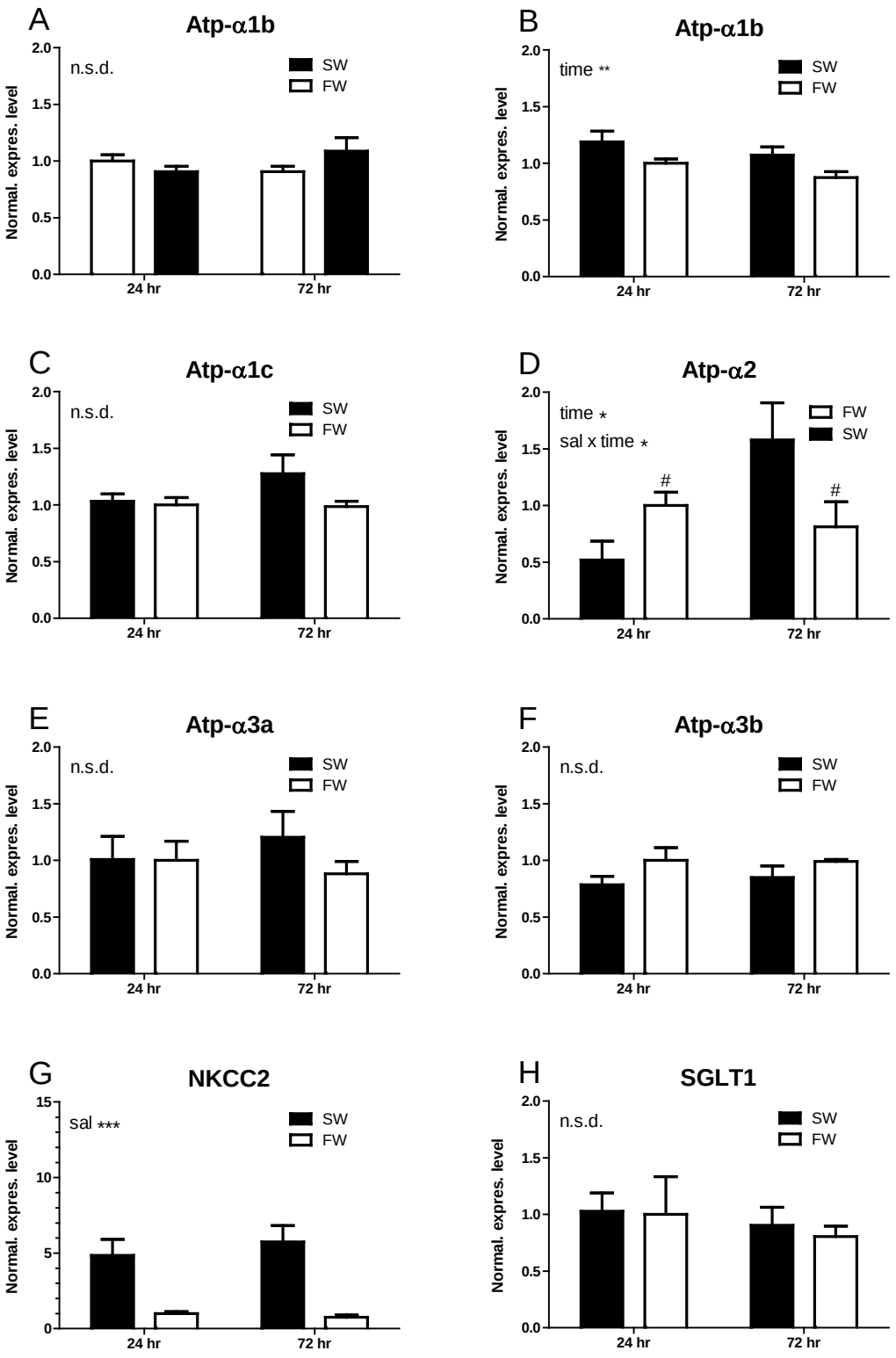

1026 **Figure 6**

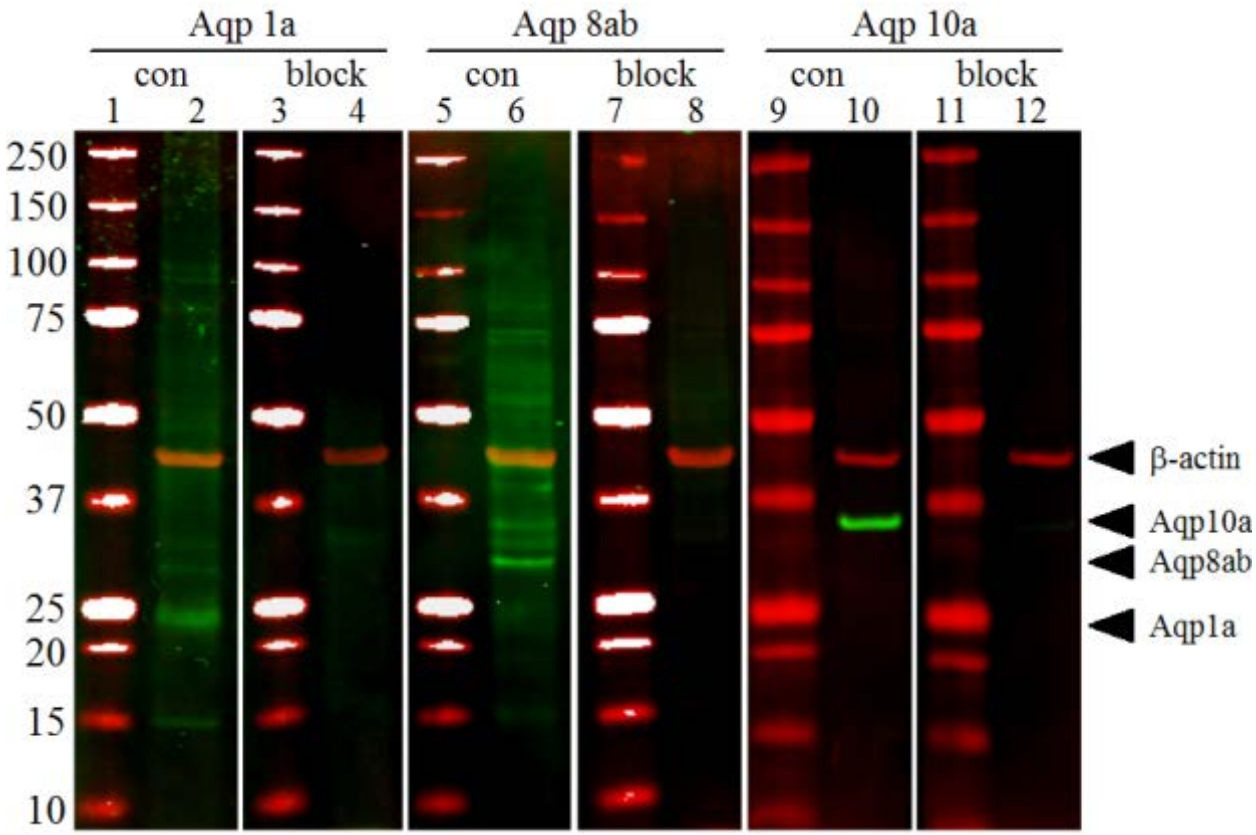

1027

1028

1029 **Figure 7**

1030

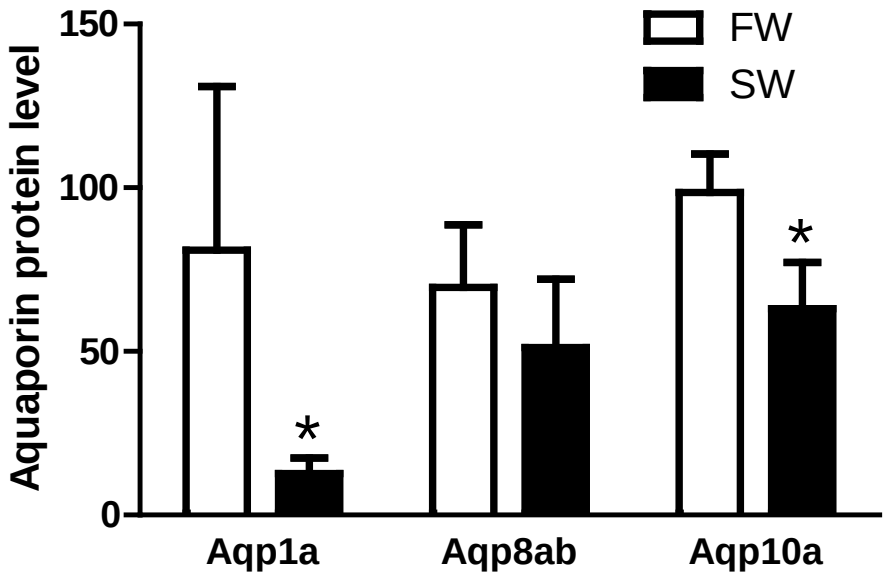

1031

1032

1033 **Figure 8**

1034

1035

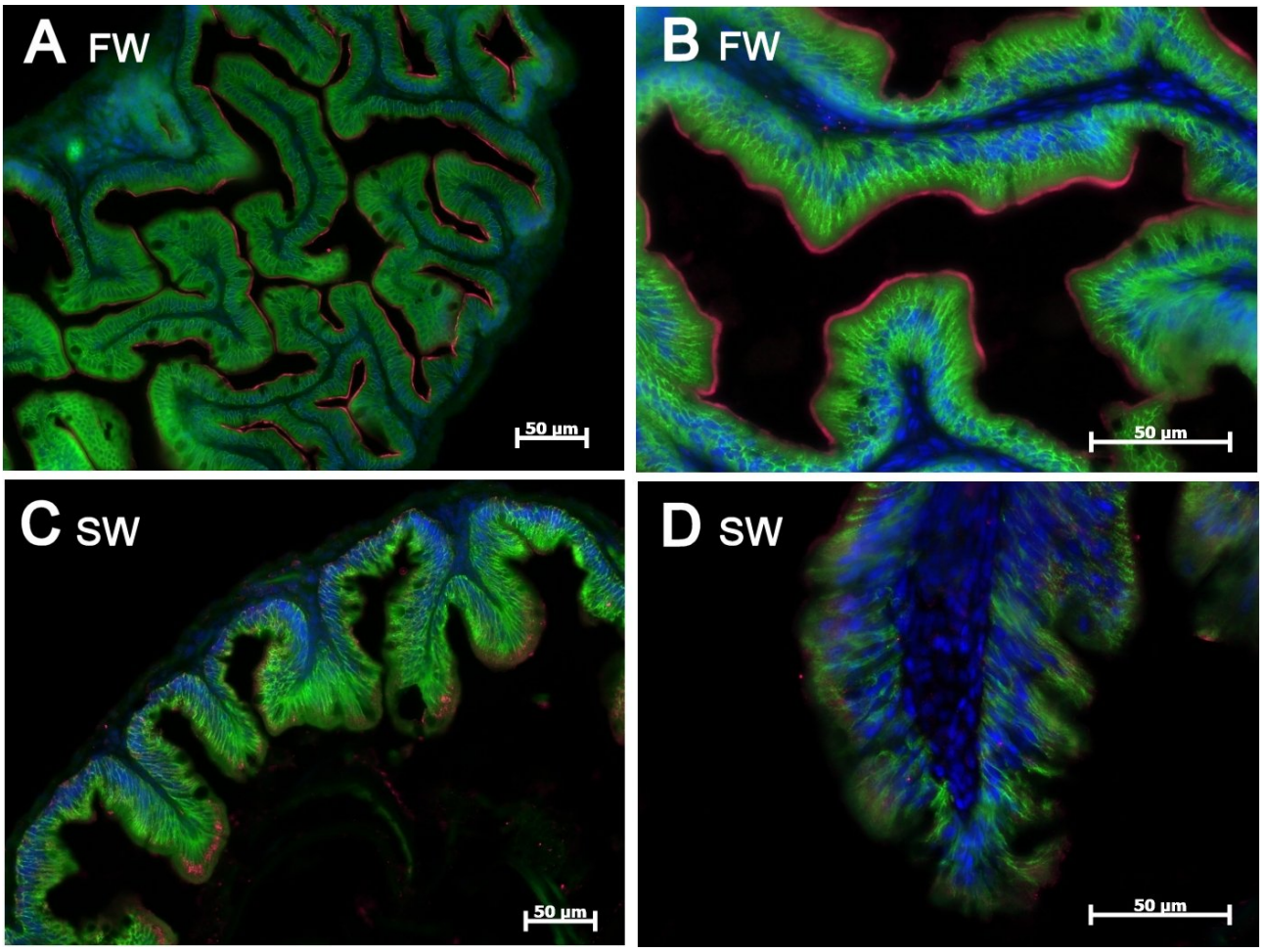

1036

1037

Figure 9

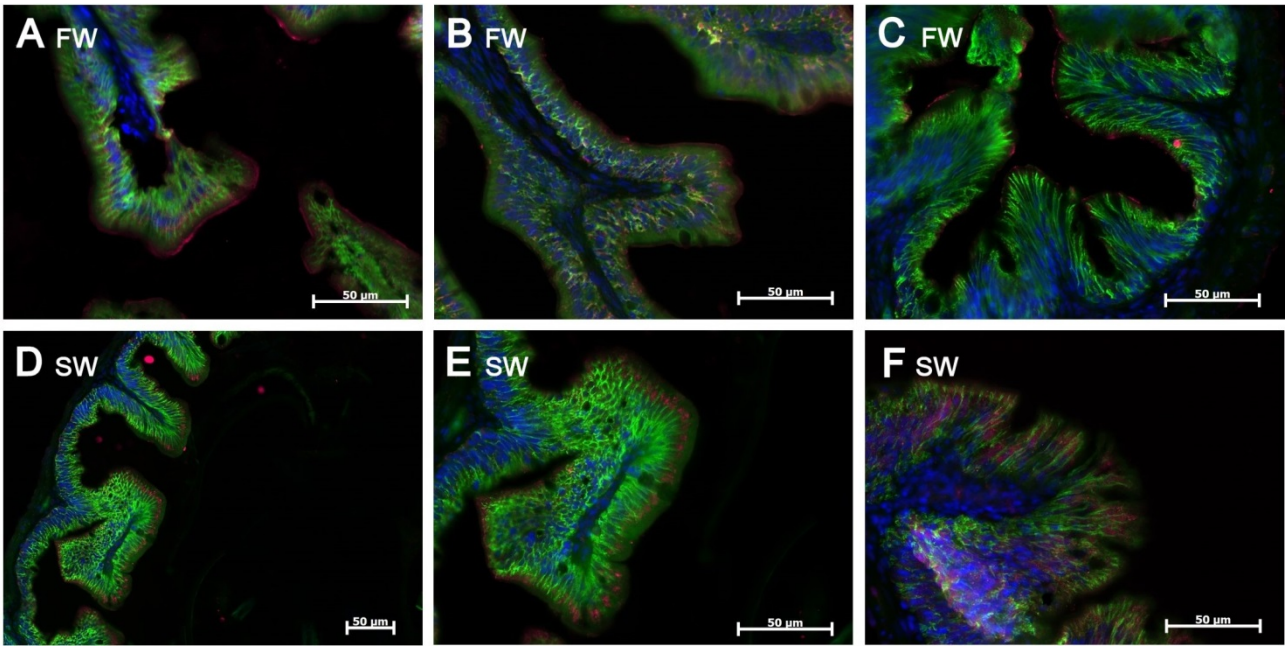

1043 **Figure 10**

1044

1045

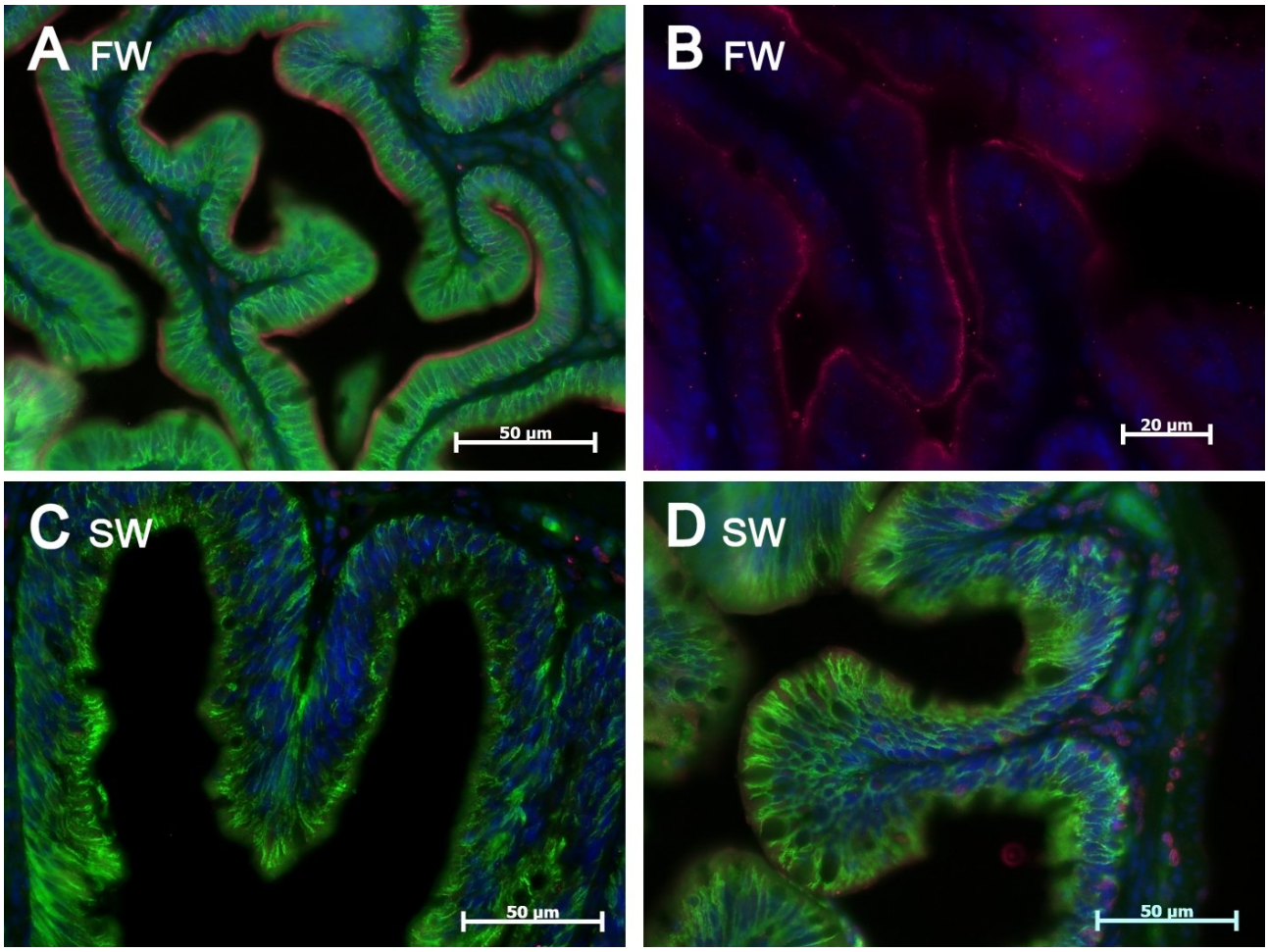

1046